**Natural Hazards
and Earth
System Sciences**

A "simulation chain" to define a Multidisciplinary Decision Support System for landslide risk management in pyroclastic soils

E. Damiano[1]**, P. Mercogliano**[2]**, N. Netti**[3]**, and L. Olivares**[1]

[1]Department of Civil Engineering – Second University of Naples, Aversa (CE), Italy
[2]CMCC – Mediterranean Centre for Climate Change, Capua, Italy
[3]Department of Economics – University of Naples "Federico II", Naples, Italy

Correspondence to: N. Netti (netti@unina.it)

Abstract. This paper proposes a Multidisciplinary Decision Support System (MDSS) as an approach to manage rainfall-induced shallow landslides of the flow type (flowslides) in pyroclastic deposits. We stress the need to combine information from the fields of meteorology, geology, hydrology, geotechnics and economics to support the agencies engaged in land monitoring and management. The MDSS consists of a "simulation chain" to link rainfall to effects in terms of infiltration, slope stability and vulnerability. This "simulation chain" was developed at the Euro-Mediterranean Centre for Climate Change (CMCC) (meteorological aspects), at the Geotechnical Laboratory of the Second University of Naples (hydrological and geotechnical aspects) and at the Department of Economics of the University of Naples "Federico II" (economic aspects). The results obtained from the application of this simulation chain in the Cervinara area during eleven years of research allowed in-depth analysis of the mechanisms underlying a flowslide in pyroclastic soil.

1 Foreword

Landslides represent one of the world's major natural hazards. In recent decades, researchers from distinct disciplines (geology, hydrology, hydrogeology, geotechnics, economics and sociology) have channelled much of their effort towards landslide risk assessment (Carrara and Merenda, 1974; IUGS, 1997; Guzzetti, 2000; Vaunat and Leroueil, 2002; Alexander, 2005; Guzzetti et al., 2005; Picarelli et al., 2005; Gamper et al., 2006; Fell et al., 2008, among others). The goal of this research activity is landslide risk analysis. The analyses can be considered quantitative only if they contemplate an exact definition of the failure mechanisms, the probability of occurrence, the run-out of the potential body, exposed property, vulnerability, damage and total potential loss (including casualties).

Focusing on the first two points, we should not underestimate the efforts made in this multidisciplinary field with regard to landslide inventories based on geomorphologic concepts, historical data, aerial photographs and satellite observations (Varnes, 1984; Wieczorek, 1984; McCalpin, 1984; Carrara et al., 1991, 1995; Fell et al., 1996; Carrara and Guzzetti 1995; Cardinali et al., 2002; Hungr et al., 1999). These studies have spawned many approaches and models for rainfall-induced landslide risk assessment: mixing objective and subjective data, they have led to qualitative, semi-quantitative or quantitative evaluations (De Graff and Canuti, 1988; Hollingworth and Kovacs, 1981; Montgomery et al., 1991; Montgomery and Dietrich, 1994; Carrara and Guzzetti, 1995; Iverson, 2000; Baum et al., 2002; Corominas et al., 2003; Crosta and Frattini, 2003; Savage et al., 2004; Revellino et al., 2004; Lida, 2004; Cascini et al., 2005; Picarelli et al., 2005, Evans et al., 2005; Rosso et al., 2006; D'Odorico et al., 2001; Picarelli et al., 2008a; Cascini et al., 2010). (A comprehensive review of these models is given in the deliverables of the Safeland Project, 2011).

Any approach presents advantages and/or constraints. A first type of constraint is imposed by the reference scale. The reference scale for the analysis (1/25 000; 1/5000; 1/2000; 1/1000; 1/500) and the corresponding study area (from a fraction of one km^2 (slope scale) up to hundreds of km^2 (basin and regional scale)) are extremely variable, and play a major role. A second constraint is imposed by the type of soil deposits and the kind of geomaterial involved in the failure and evolution mechanisms (for example, the cases of saturated soil are treated differently from the cases regarding unsaturated soil; granular deposits are analysed differently from the case regarding fine-grained deposits).

For the large-medium scale, statistical approaches (Carrara and Guzzetti, 1995) or classification based on lithology, landform or geological structure (Hollingworth and Kovacs, 1981; Montgomery et al., 1991; De Graff and Canuti, 1988; Corominas et al., 2003) have mainly been used. At a smaller scale (basin scale) and with information on soil deposits increasingly available, physically based approaches have been adopted as a combination of hydrological and geotechnical models (Lida, 2004; Rosso et al., 2006; D'Odorico et al., 2001; Crosta and Frattini, 2003; Montgomery and Dietrich, 1994; Baum et al., 2002; Savage et al., 2004).

Slope response to rainfall at regional and basin scale is generally performed on grid-based GIS technology, combining simplified hydrological models with stability analyses in the hypothesis of an infinite slope adopting the Mohr-Coulomb failure criterion or the extension for unsaturated soil. Many of the hydrologic approaches in question analyse 1-D or pseudo-3-D infiltration. Some models consider only vertical steady-state conditions with an impervious base in equilibrium with the steady-state water flow parallel to the slope. Others examine transient regimes solving the flow equation for saturated soil in the case of an impermeable basal boundary at a finite depth or of a pervious base specifying outflow rates. Other more complex hydrological models assume a simplified 1-D or 3-D transient regime, implementing the flow equation for unsaturated soil, using the well-known expressions for the soil water characteristic curves (Van Genuchten, 1980; Gardner, 1958; Brooks and Corey, 1964) and assuming as boundary condition the water inflow and outflow or values of pore fluid pressure (positive pore water pressure or suction).

Looking at the limitations of these hydrological models, the assumption of steady-state is generally highly unrealistic. This always imposes a model calibration and is suitable only in the case of continuous precipitation and when the uppermost part of the slope, located above the groundwater surface, is fully saturated and very stiff (fine-grained deposits). Vertical infiltration combined with an impervious base generates a strong constraint for long-lasting infiltration analyses. The concept of "critical rainfall" is strictly linked with the hypothesis on boundary and initial conditions. Another limitation of the models for saturated soil derives from their use in cohesionless granular deposits, as their application is not suitable for slope angles (α) steeper than saturated soil friction angle (ϕ'). These models can be used only by introducing a constant "fictitious" cohesion which strongly influences the results of the analyses. Done like this, even with the correct calibration with respect to past landslides, if these models are exported to cases which differ from that used for calibration, they generally produce a biased estimation of stability conditions.

In the case of shallow unsaturated pyroclastic deposits, the "response time" of slopes subjected to infiltration processes is a function of initial water content and capillary height distribution and can range from a few hours, in the case of
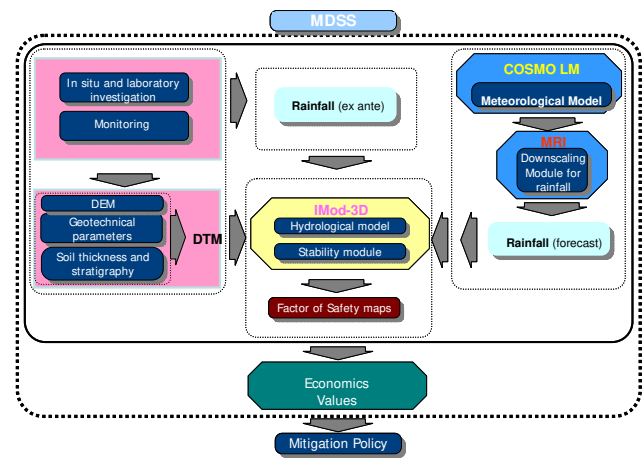

Fig. 1. Flow chart of the Multidisciplinary Decision System (MDSS).

deposits with water content near to saturation, up to several months, in the case of low saturation degree. Therefore, in the case of unsaturated pyroclastic deposits, accurate analyses may be made only by using hydrological models that remove simplified assumptions in constitutive relationships (mechanical constitutive relationships and hydraulic characteristic curves), and allow the application of realistic initial and boundary conditions. Clearly, the more complex the constitutive model, the more complex the analysis and knowledge of soil properties.

In conclusion, we believe that, to analyse steep slopes ($\alpha > \phi$') in unsaturated cohesionless pyroclastic deposits subjected to long-lasting infiltration processes, there are several reasons to propose an MDSS (Fig. 1) containing a GIS-based hydrological 3-D model.

2 Flowslides in pyroclastic soils

In recent decades a number of catastrophic flowslides have threatened and partly destroyed small towns in the foothills of Campania's Apennines in southern Italy. The most severe events, in terms of injuries and fatalities, were those which occurred in Sarno (1998), Quindici (1998), Bracigliano (1998) and Cervinara (1999) (Del Prete el al., 1998; Cascini et al., 2000; Revellino et al., 2004; Di Crescenzo and Santo, 2005; Picarelli et al., 2008a; Picarelli et al., 2008c; Cascini et al., 2010). These devastating flowslides mainly involved unsaturated cohesionless pyroclastic deposits and ran for tens of kilometres.

Detailed studies at the slope scale revealed the triggering mechanisms of those catastrophic events. These studies were based on the utilization of advanced numerical codes, both commercial and in-house. Moreover, they took into account some predisposing factors, which are sometimes undervalued, such as stratigraphic details (Picarelli et al., 2004;

Crosta and Dal Negro, 2003), vegetation, land use, cuts and roads along the slopes (Guadagno et al., 2003), springs and morphological cuts (Cascini et al., 2010, 2011).

Only recently, Damiano and Olivares (2010) added information intended to aid the authorities involved in land management in the southern Apennines to detect cases in which rainfall-induced slope failure may turn into flowslides. They stressed the mechanisms of how landslides evolve into flowslides (Olivares and Damiano, 2007), stressing the role played in failure by hydrological and geotechnical variables such as water content, degree of saturation and suction. Leroueil (2004) and Picarelli et al. (2008a) showed that a landslide evolves into a flowslide only when an undrained unstable response is established. A necessary condition for an unstable post-failure response to happen is that the soil is susceptible to liquefy and instability occurs near to saturation (Olivares, 2001).

Landslides such as slides and avalanches move at lower velocity and have a shorter run-out than flowslides. Sometimes such kinds of landslides, unlike flowslides, stop along the slope or at its toe (Picarelli et al., 2008a, b and c). The simplified framework to predict the slope response at basin scale proposed by Damiano and Olivares (2010) is reported in Fig. 2. Implementing this framework in our MDSS, we add to the detection of a landslide useful information on the spatial distribution of the hydrological and geotechnical variables. Such information is of extreme importance so as to exclude the cases of landslides that will not evolve into catastrophic flowslides and to allow the authorities involved in land management (such as the Campania river basin authorities) to reduce the occurrence of "false alarms".

3 Socio-economic perspective

The stability of slopes is, from a socio-economic perspective, a public good which is both non-rival in consumption and non-exclusive. Since there is no market in which the allocation of resources is decided, it is the state that makes this decision. Yet protective measures against rainfall-induced landslides entail complex choices. The opinions of multidisciplinary groups of experts are needed: matters of a diverse nature – civic, geological, geotechnical, meteorological, legal, economic, ecological and social – have to be considered as a whole. Moreover, tools and choices affect different stakeholders: politicians, producers, consumers, taxpayers and voters.

We believe that supporting government in mitigation policy of the risk involved in rainfall-induced landslides with scientific approach is, above all, a matter of decency and morality.

However, rationally defined safety standards must be constantly validated. In recent decades, the energies of researchers from distinct disciplines have been channelled into
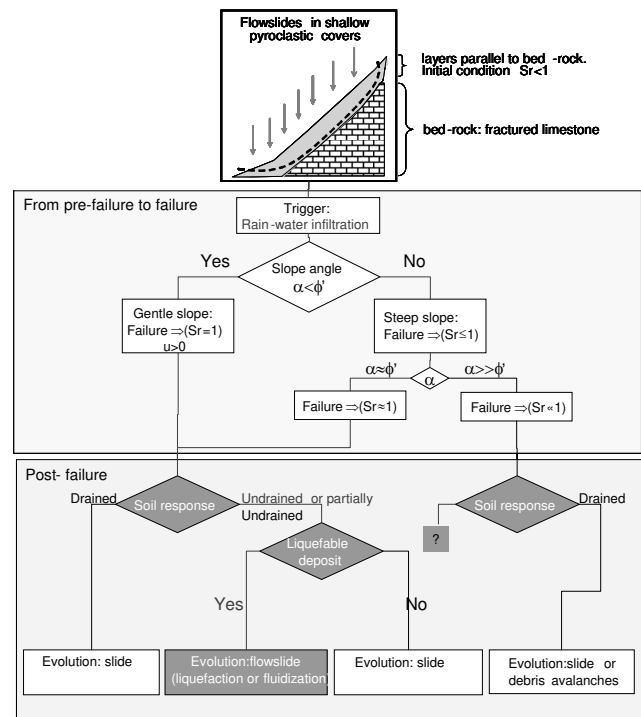
Fig. 2. Conditions for rainfall-induced flowslide in unsaturated soils (infinite slope).

landslide risk assessment. Enormous scientific progress has been reached in the case of rainfall-induced landslides.

From a socio-economic point of view, landslides are the most critical hazard for casualties and economic losses. Economic losses may reach 1 or 2 % of the gross national product in many developing countries (Vaunat and Leroueil, 2002). Large economic losses may be both the direct effect of landslides (especially in the case of "missed alarms") and the indirect effect of "false alarms" of landslides. For example, business interruptions may happen in both cases; they can result from direct property damage or from a forced shutdown produced by the electricity and/or water supply being cut off, even due to a "false alarm".

Business interruptions produce a negative chain reaction: "stock losses" such as property damage, indirectly produce "flow losses" such as decreases in production, sales, profits and wages, and job losses, as well as increases in the relative cost of social safety nets and insurers' liabilities. The total sum of indirect effects is often a "multiplier" of the direct effects of a business interruption, however it may have happened (Rose and Lim, 2002). Public policy may help in terms of "resiliency", that is the ability of individual and communities to cushion losses. Losses can be minimised (ex-ante) by providing information and (ex-post) by substituting public services for private ones, maintaining civil order, providing social safety nets, health services and financial assistance for recovery and reconstruction.

Over the past few decades, governments, environmental and research organizations worldwide have invested resources in assessing land susceptibility and its zonation (Guzzetti, 2006). Landslide mapping and detailed national geomorphological inventories are the main outputs of literature on landslide susceptibility.

Civil protection agencies and basin authorities, engaged in land monitoring and management, have issued their warnings essentially on the basis of valuable data from surveyed landslides all over Italy. Moreover, by means of statistical series of rain events, "critical thresholds" are defined. Generally, it is in respect of these thresholds that the population is alerted from time to time.

In some circumstances the early warning system fails its mission and – unfortunately – the direct costs of such a failure can be directly measured ex-post. However, in some other circumstances, "false alarms" occur. This is often due to biased estimations of stability conditions produced by inappropriate generalisations of some simplified models whose main weakness concerns the study of infiltration processes in the soil (see the Introduction). According to economists, the cost of a "false alarm" is no small matter.

To understand these losses we can refer to the economics literature of uncertainty and information and to financial literature (Von Neumann, Morgenstern, 1944; Pratt, 1964; Hanoch and Levy, 1969; Rothschild and Stiglitz, 1970; Marschak and Radner, 1972; Guiso and Terlizzese, 1994, amongst others). Market risk premiums are strictly dependent on expectations of losses. Financial market operators, such as insurance companies, base risk transfer premiums offered against landslides on probability distributions of the catastrophic events.

Information can be more or less precise. Sources of information based on past observations are highly valued and obviously cannot be neglected. The aim of our Multidisciplinary Decision Support System (MDSS) in the near future will be to link measured rainfall (input) to the effects in terms of infiltration and slope stability and ultimately arrive at a definition of vulnerability and risk assessment (Fig. 1). This "simulation chain" will add the rainfall forecasts of the meteorological models as new inputs for slope response analyses.

As future perspectives, meteorological, geological, hydrological and geotechnical outputs of such an MDSS will help estimate probabilities of rainfall-induced landslides conditional upon constantly updated information. Conditional probabilities obtained could be inputs for vulnerability and risk assessment and for monetization of risks (Chung and Fabbri, 1999; Gorsevski et al., 2003; Guzzetti, 2006; Alexander, 2005).

We believe that adoption of our approach will help reduce the cases of failure in early warning systems, "false alarms" and market risk premiums, and will support private and public decisions about whether and where to allocate resources to cope ex-ante with rainfall-induced landslides.

4 The core of the Multidisciplinary Decision Support System (MDSS)

The core of the MDSS consists of algorithms and software to be used for the analysis of hydrological phenomena, in particular shallow landslides caused by intense precipitation, and then to predict such events using a "simulation chain" of the different physical phenomena mentioned. In this paper we define and validate tools for this purpose. The MDSS requires the development of computational weather models which can satisfactorily anticipate the evolution of the synoptic weather and its changes due to interactions with the Earth's surface and in particular the rainfall pattern, especially for very intense events. However, it is also important to be able to "concatenate" the results of the weather forecast models with the analysis of the effects of extreme rainfall on the ground in terms of rainfall infiltration and slope stability. Therefore, it is very important to develop and optimise mathematical models in such a way that they become more accurate, robust and efficient, but also to define an interface between the different models. Construction of this "simulation chain" is a high priority because landslides usually occur on very limited areas (slope scale), while the numerical weather forecasts currently used operatively, albeit using very high resolution models, are defined on much larger scales (mesoscale, of the order of kilometres). The developed MDSS is able to produce appropriate results in brief computational times, in order to be used operatively by the agencies responsible for civil protection. This means always having output available in short computational times and an immediate interpretation output. During our activity, it was discovered that the best approach to the problem is to establish a multidisciplinary team, which would simultaneously address the issues from different points of view, providing constant comparison and integration of the different skills.

Below the various components of the MDSS are presented (Fig. 1): the weather model for the atmosphere (COSMO-LM), the downscaling module (MRI) and the hydrological/geotechnical model for saturated-unsaturated soils associated to the module for stability analyses (I-MOD3-D). The code for weather simulations (COSMO-LM) is used to define the boundary condition for the hydrological/geotechnical model (I-MOD3-D) through a downscaling module (MRI). The results of the MDSS initialized on observed data in 2006 are reported.

5 Meteorological model (CMCC)

The code employed for weather simulations is the COSMO-LM model (Doms and Schattler; 1999, 2002). This model is developed by the European "Consortium for Small-Scale Modelling" COSMO (www.cosmomodel.org). The consortium is nowadays formed by different national weather services and research centres within the member countries. In

particular, the Italian Air Force, regional agencies for environmental protection (ARPA Emilia Romagna and Piedmont) and CMCC represent the Italian components of the Consortium. COSMO LM is developed and used operatively by the meteorological services of several European countries, namely Germany, Greece, Italy, Poland, Romania, Russia and Switzerland. Currently, the Italian version of COSMO LM, called LAMI, is the reference model for the Italian Civil Protection (Prime Minister's Directive; 2004). All the operative centres of the Italian Civil Protection, in particular, receive data from this model on a daily basis.

COSMO-LM is a non-hydrostatic limited area atmospheric prediction model; it is based on primitive thermohydrodynamic equations describing compressible flow in a moist atmosphere. The model equations are formulated in rotated geographical coordinates and a "generalized terrain following height coordinates". The "generalized terrain following height coordinates" is the usual choice for the meteorological model. This system was defined by Phillips (1957) with the goal of defining a coordinate surface coincident with the bottom orography. This feature permits a more efficient use of the computer resources and simplifies the application of the lower boundary conditions (Clark, 1977). A variety of physical processes are taken into account by the parameterization scheme (grid scale cloud and precipitation, moist convection, radiation, soil model, surface layer and subgridscale turbulence).

In the soil module of COSMO LM, called TERRA_LM, the equations of mass conservation and heat conduction are implemented among soil, vegetation and atmosphere (Heise et al., 2006; Doms et al., 2005). TERRA_LM is a Soil-Vegetation-Atmosphere-Transfer (SVAT) model simulating heat and humidity fluxes between soil and atmosphere surfaces. SVAT models have been widely used in recent years in both biophysics and ecology to determine vegetation behaviour when faced with extreme conditions, coupled with models of flood prediction to determine water volume.

The prognostic variables of the COSMO LM model are horizontal and vertical Cartesian wind components, pressure perturbation, temperature, specific humidity, cloud water content and optionally cloud ice content, turbulent kinetic energy, specific water content of rain and snow.

The tool described in this paper to evaluate stability analysis following intense rainfall uses data from this meteorological model. Besides, COSMO LM is the meteorological model operatively used by the Italian National Weather Service to predict weather and flood occurrences. This means that the meteorological data of COSMO LM are available on a daily basis, providing the input for the simulation chain described in this paper. This opportunity also means that every day it is possible, using the rainfall forecasted by COSMO LM, to run the simulation chain proposed herein in order to validate it. The early warning procedure is reported in Fig. 3. In Fig. 4 we illustrate the domains of the two different configurations of COSMO-LM LAMI operatively used in Italy.
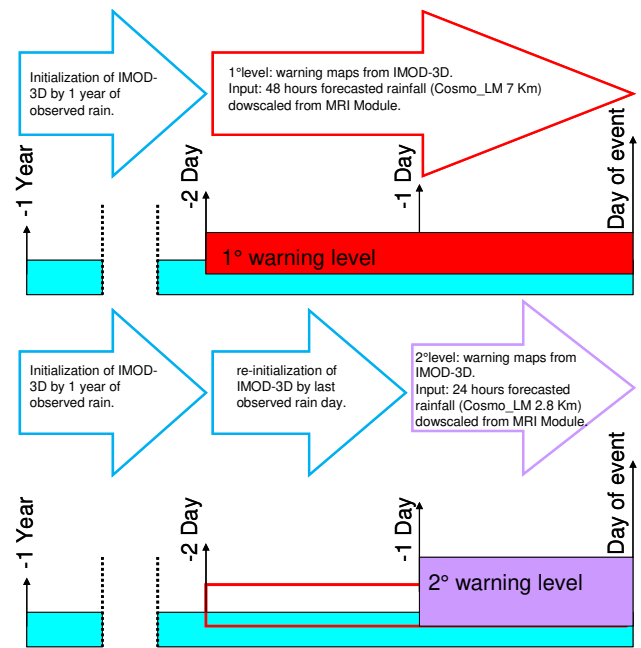

Fig. 3. Warning procedure for the evaluation of the shallow landslide risk.

The two different configurations have different spatial resolutions, 7 and 2.8 km respectively, and two different forecast time ranges, 72 h and 48 h respectively.

The model time steps are 40 s for COSMO LM, with the horizontal resolution of 7 km, and 10 s for COSMO LM with the horizontal resolution of 2.8 km. Different time steps can also be selected (see http://www.cosmo-model.org/content/tasks/operational/default.htm). The time step is the period for the integration of the numerical equations. The output fields of COSMO LM are produced every 3 h for COSMO LM 7 km and every 1 h for COSMO LM 2.8 km. This is the time period in which the forecast skill is better (this is related to the horizontal scale; Doms et al., 2011). The configuration with a 7 km resolution has a bigger domain with respect to the configuration with a horizontal resolution of 2.8 km. Since these two model configurations are able to calculate the evolution of the atmospheric variables only in a small portion of the Earth, due to existing computer power, they are called limited-area models (LAMs). LAMs provide forecasts on a smaller area than the global model but with a higher spatial (from 1 to 10 km) and temporal (from 1 to 3 h) resolution. The development of LAMs has responded to the need to push model resolution up to cells of a few kilometres, especially to predict precipitation where there are many processes involved, ranging from synoptic scale to mesoscale, including processes in the planetary boundary layer and microphysical processes, which interact with each other. Orography introduces further complexity, leading to a change in the dynamics and microphysics, not only in proximity of the
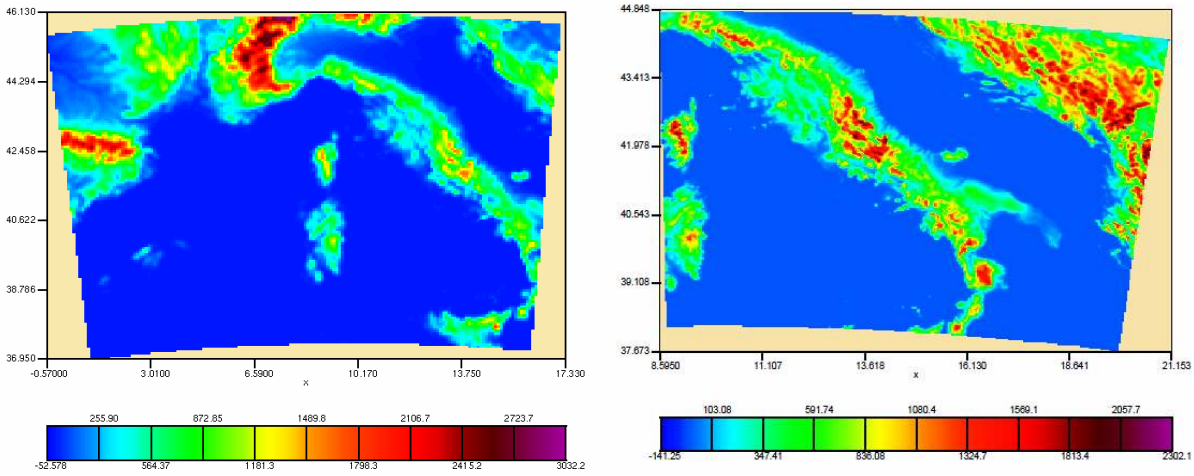
Fig. 4. Domains used in COSMO-LM for the evaluation of atmospheric variable; **(a)** 7 km; **(b)** 2.8 km.
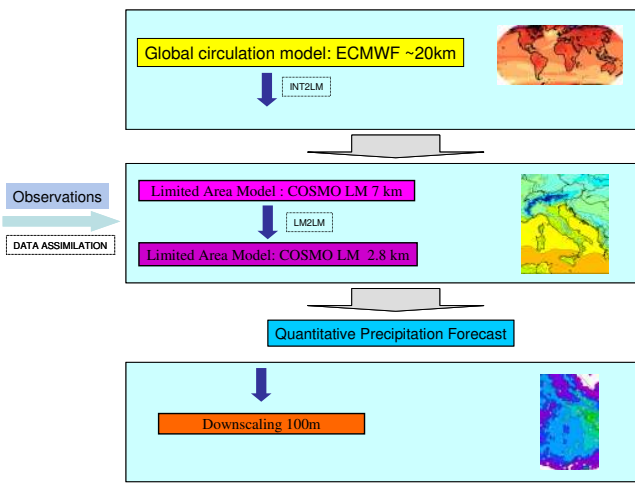

Fig. 5. Meteorological model steps.

relief but also at a distance which is sometimes considerable. In terms of modelling, suitable representation of orography and of related small-scale processes has yet to be found. Currently, the mesoscale models are those best able to assess some high-impact events such as small hurricanes, storms and very extensive tornadoes (Trentmann et al., 2009).

LAMs need to be initialized by global models through proper initial and boundary conditions. Regional models represent a dynamic downscaling of global circulation models (GCMs). Initial and boundary conditions to the LAM models can also be provided by a lower resolution LAM. GCMs are numerical models providing forecasts on the entire globe. Due to existing computer power, they have a resolution of about 15–20 km and a forecast time range of about 10 days. To improve the GCM forecast resolution, the GCM forecast data are used as initial and boundary conditions

for COSMO-LM 7 km. At this point the forecast data of COSMO LM 7 km provide initial and boundary conditions for COSMO LM 2.8 km. This simulation chain enables the atmospheric model to provide forecasts at the resolution of 2.8 km. For the implementation of the simulation chain proposed in this paper (Fig. 5) the ECMWF (European Centre for Medium-range Weather Forecast) spectral global model, termed Integration Forecast System (IFS) (Simmons, 1989), is used to provide initial and boundary conditions for the COSMO-LM regional model at a horizontal resolution of 7 km. COSMO LM initial conditions are provided by interpolating initial data from IFS and from the continuous data assimilation stream. Explicit balancing by a hydrostatic temperature correction for surface pressure updates, a geostrophic wind correction and a hydrostatic upper-air pressure correction are also provided by the nudging procedure. The initial conditions are calculated by the pre-processing program INT2LM. A detailed description of interpolation procedures is provided on the COSMO web site (Schaettler, 2009). The lateral boundary conditions are obtained with a one-way nesting by Davies-type lateral boundary formulation (Davies, 1976, 1983). The top boundary conditions are represented by a rigid lid condition and a Rayleigh damping layer (Torrisi, 2005). The latter is an absorbing layer used to reduce spurious downward reflection of vertically propagating waves from the rigid top boundary, which can completely distort the numerical solution. This viscous damping layer is usually applied at the top of the computational domain to absorb upward propagating wave disturbances before they reach the rigid top boundary. Free or non-slip boundary conditions are imposed at the bottom of the boundary (for details on the boundary conditions see Doms et al., 2005).

The models used to assess slope stability require precipitation input at a scale in the order of tens or hundreds of metres: due to the impossibility of using resolutions higher than 2.8 km in numerical weather prediction (NWP) models,
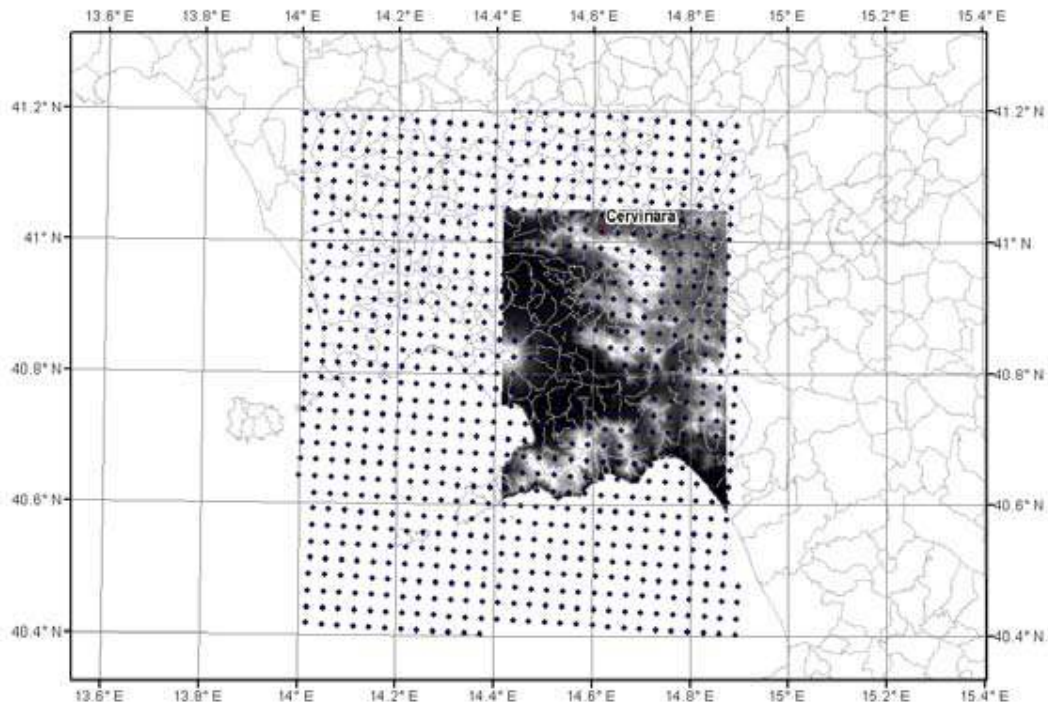
Fig. 6. Superimposition of COSMO LM 2.8 km model grid points (black dots) with the Digital Elevation Model (DEM) with the area with a finer grid resolution of 100 m × 100 m (grey scale).

the algorithm to downscale the rainfall data has to be defined, thus, allowing the two classes of models to interface.

Rainfall represents a very discontinuous meteorological variable, whose distribution is strongly affected by orography. Starting from the precipitation forecast of the COSMO LM model on the area of interest a digital model of an interpolated precipitation is defined on a regular grid with a resolution of up to 100 m × 100 m (Fig. 6). Several methods for interpolation were tested, namely Inverse Distance Weight, Radial Basis Function (RBF), Kriging (ordinary, simple, universal and disjunctive), Local and Global Polynomial Interpolation and Multivariate Regression Method (MRI) (Antofie, 2009). The best performances were obtained with a method which combines MRI and RBF.

MRI allows a regression of precipitation to be performed with respect to topographical variables (Baillargeon, 1989; Vigier, 1981) following the relationship:

To retrieve the values of precipitation at each point (i, j) of the finer grid (100 m × 100 m), the values of residuals, known only at points (m, n) of the coarser grid, were interpolated by using the RBF statistical method as proposed by Ninyerola et al. (2000) and Agnew and Palutikof (2000). Hence, the values of precipitation at each point of the higher resolution domain ($Rain_{i,j}$) can be obtained as

$$Rain_{i,j} = RBF(residuals) + a_0 + a_1 \, Elevation_{i,j} + a_2 \, Aspect_{i,j} + a_3 \, Slope_{i,j}. \qquad (1)$$

By adopting this method, only a small part of precipitation is physically interpolated by using topographic variables (MRI method) while the largest part is interpolated by using the statistical method RBF. However, even if there is little correlation between the precipitation and the topography, this method gives numerical stability to the hydrological/geotechnical model put in cascade simply because it actually takes into account the features of the topography. To date, no technique for the temporal downscaling of precipitation has been tested. This is due to the nature of the hydrological-geotechnical model that does not require an input with a time resolution smaller than one hour.

This procedure was implemented as a plug-in module for ArcGIS that automatically elaborates fine resolution precipitation data (rasters) based on hourly precipitation forecast. The calculated ArcGIS raster data is directly read by the stability model in cascade.

6 Hydrological/Geotechnical model – I-ModGIS 3-D

I-MOD 3-D is a 3-D finite volumes code for infiltration and stability analysis developed at the Geotechnical Laboratory of the Second University of Naples (Olivares and Tommasi, 2008; Damiano and Olivares, 2007, 2010; Olivares et al., 2009). The goal of the I-MOD 3-D code is to define a warning map at the basin scale in loose unsaturated pyroclastic
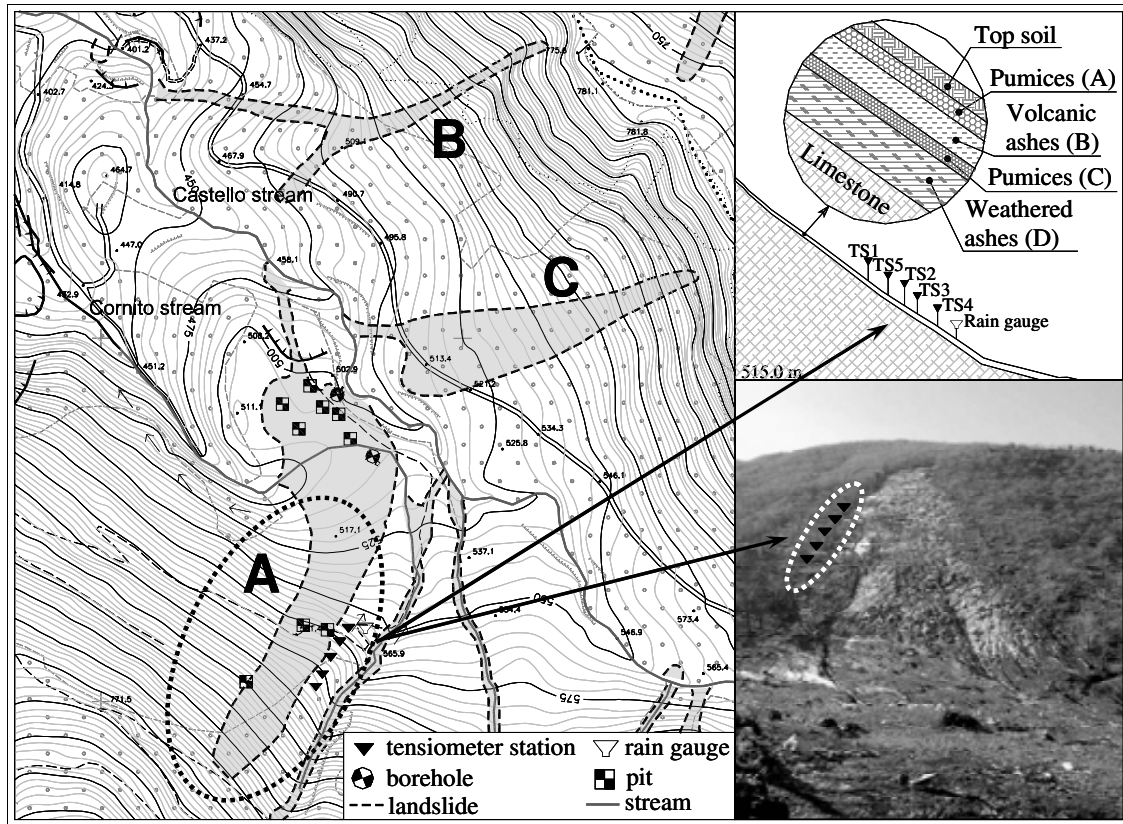
Fig. 7. Cervinara site: plan-view, monitoring station and schematic cross-section.

soils. This code represents the "last link" of the "simulation chain". This component of the chain consists of a finite volume model for infiltration analyses (I-MOD3-D) and a stability module which has respectively the goal of analyzing the rainfall-induced infiltration process (definition of spatial-temporal distribution of suction, water content and degree of saturation) and assessing the stability conditions of shallow deposits (definition of a stability map). These two parts are integrated through an interface able to automatically define a finite volume discretization of soil starting from a digital terrain model (DTM), and to capture the forecasted rain from the MRI module.

The 3-D finite volumes module for infiltration analysis is developed as a visual basic application (VBA) for ARC-GIS 9.2 in an uncoupled formulation for unsaturated porous media in isothermal conditions, neglecting the flux of the gas phase. The current version of this module does not consider run-off or vegetation (transpiration). Mesh-generation automatically starts from the digital terrain model. The general governing differential equations for 3-D flow are expressed as

$$\bar{v}(x,y,z,t) = -K\left(\theta(x,y,z,t)\right) \times \nabla(\psi\left(\theta(x,y,z,t)\right) + z) \quad (2)$$

$$\frac{\partial \theta(x,y,z,t)}{\partial t} = -\nabla \times \boldsymbol{v}(x,y,z,t) \quad (3)$$

where:

$\theta(x,y,z,t)$ is the volumetric water content;

$v(x,y,z,t)$ is the velocity x,y,z;

$K(\theta(x,y,z,t))$ is the hydraulic conductivity;

$\psi(\theta)$ is the relationship between capillary pressure head (fluid pressure potential) and volumetric water content (WRC water retention curves) in unsaturated soils. The water retention curves ($\psi(\theta)$) are described by the Van Genuchten expression (1980):

$\theta = \theta_{\mathrm{r}}(\theta_{\mathrm{s}}\theta_{\mathrm{r}})/[1(\alpha\psi(\theta)^n)]^m$

where:

θ_{r} is the residual volumetric water content;

θ_{s} is the saturated volumetric water content;

α, n, m are parameters estimated from experimental measurement.

The hydraulic conductivity functions implemented in the model are both the Van Genuchten (1980) and the Brooks and Corey (1964) relationships, depending on volumetric water content θ and porosity n or degree of saturation S_{r} ($\theta = nS_{\mathrm{r}}$):

$k = k_{\mathrm{sat}}\mathrm{Se}^{0.5}[1 - (1 - \mathrm{Se}^{1/m})^m]^2 \quad$ (Van Genuchten, 1980) (4)

CERVINARA a)

- DEM $\Delta x = \Delta y = 5$ m b)

- homogeneous unsaturated porous media

- saturated permeability:
  $5 \cdot 10^{-7}$ m/s $< k_{sat} < 5 \cdot 10^{-6}$ m/s

- unsaturated permeability: $k = k_{sat} \cdot S_r^3$

- WRC: $\theta = \theta_r + (\theta_s - \theta_r)/[1 + (\alpha \ \Psi(\theta))^n]^m$
(van Genuchten, 1980)

- parameters:
  $0.1 < \theta_r < 0.3$; $\theta_s = 0.7$; $0.05 < m < 0.08$; $n = 20$; $\alpha = 5$

Shear strength

c)

Saturated soil:
- effective friction angle $\phi' = 38°$;
- effective intercept of cohesion $c' = 0$;

Unsaturated soil:
- effective intercept of cohesion $c' = 0$
- effective frictional angle $\varphi' = 38°$
- "apparent" cohesion $c = f(u_a - u_w)$

Fig. 8. Cervinara Digital Terrain Model (DTM).

$$k = k_{sat}[(Se)]^\delta \quad \text{(Brooks and Corey, 1964)} \quad (5)$$

where $Se = (Sr\text{-}Srr)/(1\text{-}Srr) = (\theta - \theta_r)/((\theta_s \theta_r)$ effective degree of saturation;

$\quad Srr$ = residual degree of saturation;

$\quad \delta$ = empirical constant related to the pore size distribution index.

The stability module computes for each point of the subsoil the local safety factor under the assumption of infinite slope using the following expression:

$$FS = \frac{\tau_{\lim}}{\tau} = \frac{[c' + (\psi(\theta)/\gamma_\varpi) \times \chi \, tg\phi'] + (\sigma_\beta - u_a) \times tg\phi'}{\tau_\beta} (6)$$

where: c' is the effective cohesion;

$\quad \gamma_w$ is the water specific weight;

$\quad \tau_\beta$ are the shear stresses parallel to the slope;

$\quad (\sigma_\beta - u_a)$ are the net stresses normal to the slope;

$\quad \chi$ is a parameter that describes the unsaturated shear strength increment due to the suction increase;

$\quad \phi'$ is the effective friction angle.

In this expression the shear strength of soil along planes parallel to the ground surface is calculated by means of the extension of the Mohr-Coulomb criterion for unsaturated soils (Fredlund and Rahardjo, 1993), supplied by the suction values which are calculated by I-MOD3-D. The code contains an integrated post processor to display, for each integration time and for different depths, contour maps of the volumetric water content, matrix suction and the local safety factor.

7 Test cases: description and results

To ascertain the reliability of the presented "simulation chain", we consider the well-documented case study of Cervinara, where in 1999 a landslide evolved into a catastrophic flowslide. The Cervinara study area represents a typical geomorphological context where volcanic ashes rest on fractured limestone. It is directly sited on the slope involved in the catastrophic flowslide (Fig. 7). The area has fairly regular steep slopes (around 40°) consisting of layered unsaturated air-fall pyroclastic soils in primary deposition overlying fractured limestone. In situ investigations and monitoring of suction and rainfall are available (for details see Olivares et al., 2003; Damiano and Olivares, 2010; Damiano et al., 2012) as well as mechanical and hydraulic properties of the soils (for details about experimental programmes and geotechnical models see Olivares and Picarelli, 2001, 2003; Olivares and Damiano, 2007; Greco and Guida, 2008; Greco et al., 2010).

For Cervinara, data are available from a pluviometric monitoring network of the Civil Protection. Moreover, since 2002 the monitoring system of the Second University of Naples (SUN) has been producing data from the rain gauge inside the monitoring station; as it is directly located on the slope subjected to the catastrophic flowslide, its data are preferred for the calibration of our MDSS. The landslide area was investigated with some boreholes located at the toe of the slope, and a number of shallow pits dug along the slope (Olivares et
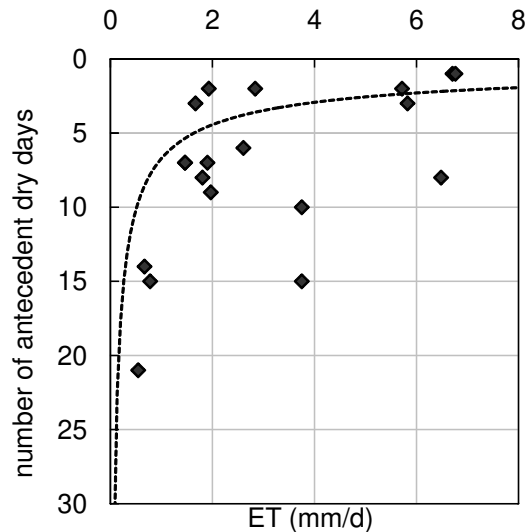
Fig. 9. Estimated evapotranspiration rate (Cervinara: 2006–2007).

al., 2003a). Consisting of cohesionless pyroclastic soils, the deposit has an average thickness of 2.4 m.

The data on slope geometry (aerophotogrammetry at a scale of 1:5000) and soil properties were combined to define the DTM in Fig. 8. The slope (about 1 km^2) was discretized in the IMOD-3-D module as a homogeneous soil with a 3-D mesh generated by DEM with a constant cell size of $dx = dy = 5$ m (using a square grid based cell) and using a constant $dz = 0.12$ m. The bedrock, constituted by fractured limestone, was assumed at a constant depth of 2.4 m.

Three events in 2007 (Table 1) were selected to test the chain. The test cases aimed to evaluate the performance of the simulation chain, comparing observed and predicted rainfall and suction in the subsoil. Even if during these events no landslide was detected, quite high cumulative rainfall was found in the rain-gauge installed at the Cervinara site.

7.1 Calibration of the infiltration model

The infiltration process was numerically simulated under the hypothesis of a homogeneous deposit for both areas and applying as ground boundary conditions the average daily rainfall intensity during rainy days (pluviometric measurements) or the evaporation flux during dry days. The evaporation flux towards the ground surface (Damiano et al., 2012) was estimated from Cervinara in situ suction measurements provided by tensiometers installed between 60 and 90 cm of depth. The calculations are based on Darcy's law and suction measurements. Hydraulic conductivity was estimated from the Brooks and Corey (1964) expression. The hydraulic flux (Fig. 9) seems to depend mostly on the number of antecedent dry days, regardless of the season (the higher the number of dry days, the lower the flux rate). The trend reported as a dotted line was assumed in numerical simulation
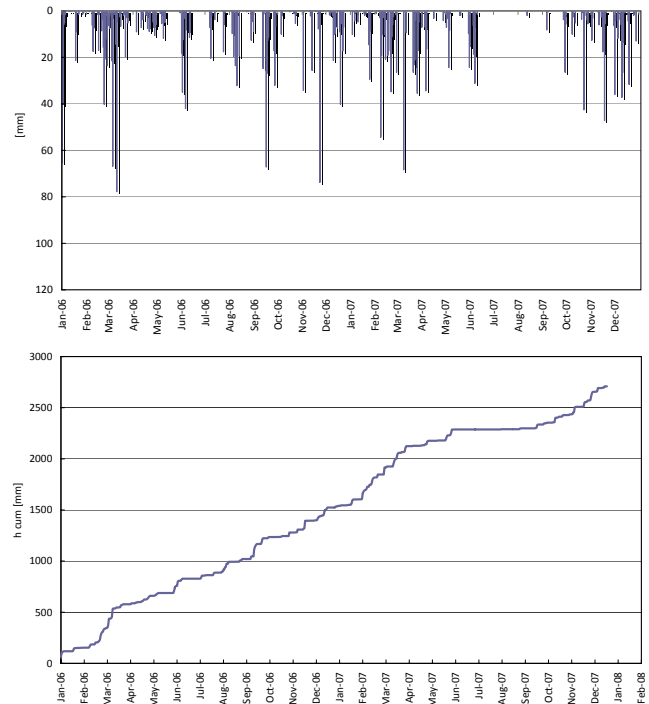

Fig. 10. Boundary conditions applied in terms of rainfall daily and cumulative height (Cervinara 2006–2007).

as evaporation flux during dry days. For the lateral and base surfaces a boundary condition of free flow was adopted.

Figures 10 and 11 show the boundary conditions applied in terms of rainfall daily height and cumulative height and of IN-OUT water flux and cumulative height balance through the soil-atmosphere interface. In 2006 the cumulative rainfall at Cervinara was about 1500 mm with a IN-OUT water flux height balance of 610 mm. In 2007 the number of dry days was lower, causing smaller differences in terms of water flux balance (IN-OUT = 260 mm) (Figs. 10 and 11).

Starting from this input in terms of water flux through the soil-atmosphere interface, the validation step consisted of a set of parametric analyses exploiting the range of variation of soil parameters obtained from laboratory tests (and reported in Fig. 8) under the assumption of a homogeneous unsaturated porous medium, assuming as initial condition a constant value of suction equal to the mean value (10 kPa) recorded at Cervinara at the beginning of the simulation (January 2006).

The best fitting of suction measurements was obtained by adopting:

- for the water retention curve the van Genuchten (1980) expression with $\theta_s = 0.7$, $\theta_r = 0.1$, $m = 0.08$, $n = 20$, $\alpha = 5$;

- for the unsaturated hydraulic conductivity functions the Brooks and Corey (1964) expression ($k = k_{sat}$

Table 1. Test cases.

| Event		Features of COSMO-LM Module	Downscaling MRI Module
From	to		
3 Apr 2007	4 Apr 2007	Hor. Res. = 7 km Forecast Time Range = 24 h;	–
3 Apr 2007	4 Apr 2007	Hor. Res. = 2.8 km (no convection); Forecast Time Range = 24 h	–
3 Apr 2007	4 Apr 2007	Hor. Res. = 2.8 km (shallow convection); Forecast Time Range = 24 h	From 2.8 km to 100 m
6 Mar 2007	7 Mar 2007	Hor. Res. = 7 km Forecast Time Range = 24 h;	–
6 Mar 2007	7 Mar 2007	Hor. Res. = 2.8 km (no convection); Forecast Time Range = 24 h	–
6 Mar 2007	7 Mar 2007	Hor. Res. = 2.8 km (shallow convection); Forecast Time Range = 24 h	From 2.8 km to 100 m
6 Feb 2007	10 Feb 2007	Hor. Res. = 7 km Forecast Time Range = 36 h;	–
6 Feb 2007	10 Feb 2007	Hor. Res. = 2.8 km (no convection); Forecast Time Range = 24 h	–
6 Feb 2007	10 Feb 2007	Hor. Res.,= 2.8 km (shallow convection); Forecast Time Range = 24 h;	From 2.8 km to 100 m
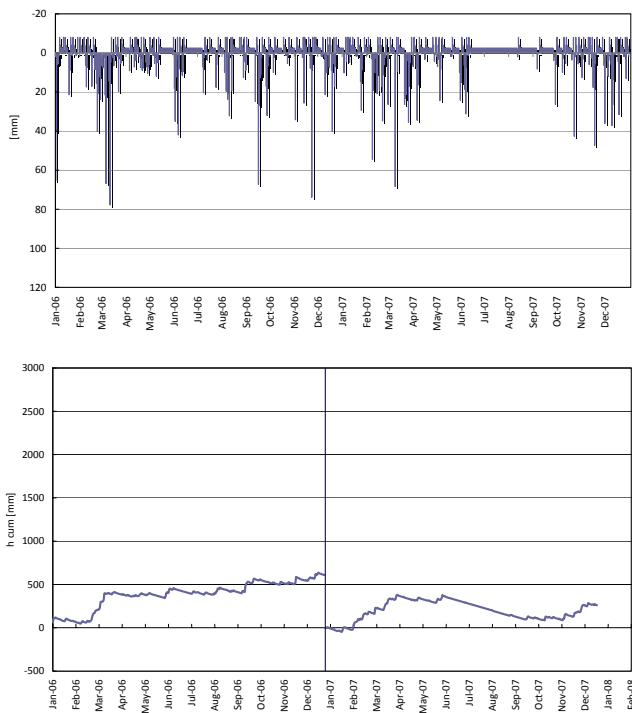
Fig. 11. Boundary conditions applied in terms of IN-OUT water flux and cumulative height balance (Cervinara, 2006 and 2007).

Fig. 12. Cervinara case: numerical simulation results; **(a)** comparison between the suction (height) measurements, rainfall and numerical data; **(b)** safety factor trend.

$(S_r)^\delta$), considering for the saturated conductivity the mean value obtained in the laboratory test ($k_{sat} = 1 \times 10^{-6}\,\mathrm{m\,s^{-1}}$) and a nil value of the residual degree of saturation Srr and an empirical constant related to the pore size distribution index, $\delta = 3$.

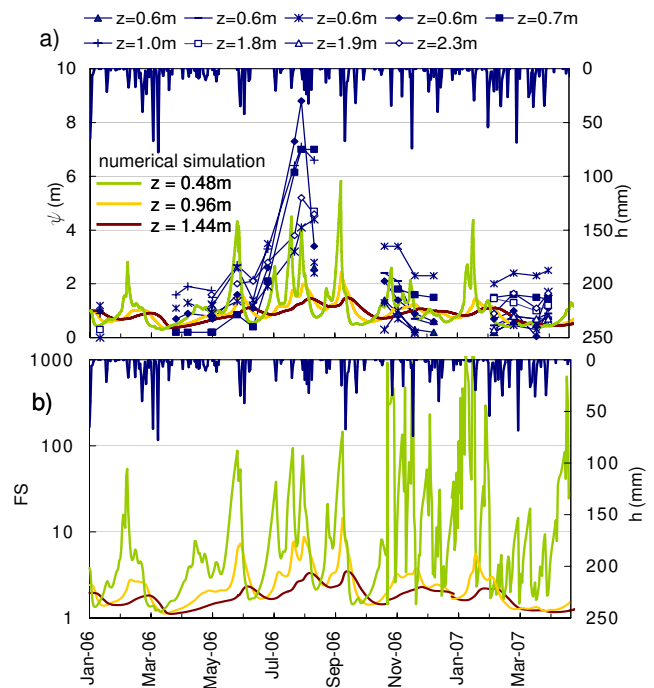In Fig. 12 we report the simulated suction trends between the depths of 0.6 m and 1.5 m (point A located along the

slope) compared with the suction measurements taken along the slope and at different depths.

Different measurements are made at different points in space at the same depth. Understandably, the spatial heterogeneity of soils produces different measurements at the same depth. In order to make a more significant comparison, the results of numerical simulation are compared with a re-elaboration of the same results considering the average
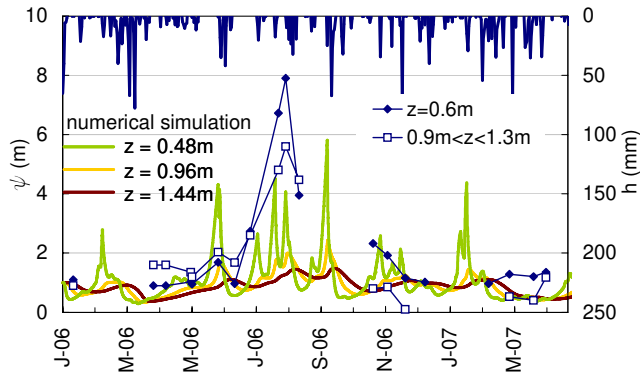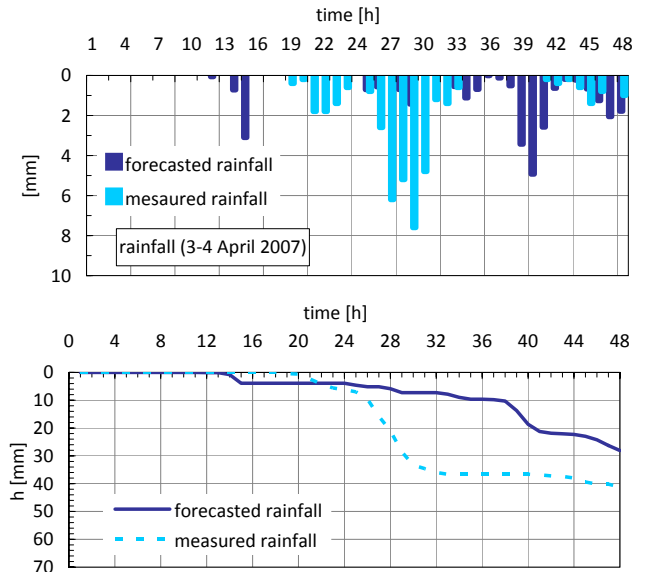
Fig. 13. Cervinara case: numerical simulation results; comparison between the mean value suction measurements (height), rainfall and numerical data.

Fig. 14. First test case: hourly rain intensity and cumulative rain height during 3–4 April 2007, evaluated at points A in the site of Cervinara.

of the different measurements (Fig. 13). Another aspect that is worth considering is that this comparison is made by considering a numerical simulation, in the hypothesis of a homogeneous soil, lasting more than 16 months; applying as boundary condition in the absence of rain the OUT water flux estimated from elaboration of the same suction and water content measurements we sought to reproduce. Hence, the results presented in Fig. 13 in the wet period have to be considered in good agreement with the numerical simulation, while during dry periods the predicted trend is to be considered "qualitatively" in agreement with measurements in the topsoil, albeit at lower values.

In our opinion, this is probably due to the combination of two factors:

– the simplified assumptions on evaporation flux applied in the model at the ground interface with the atmosphere do not take properly into account the effect of transpiration in the shallowest layer due to the presence of vegetation (brushwood and chestnut wood);

– the hydraulic conductivity function is unable to correctly simulate the unsaturated soil response in pyroclastic soil.

This last consideration is not linked to the ability of the van Genuchten expression to reproduce the functional relationship between suction and volumetric water content or degree of saturation (amply demonstrated in the literature) but, rather, to the biased estimation of hydraulic conductivity in the case of pyroclastic soils, as shown by Romano et al. (2011). This biased estimation is explained by Romano et al. (2011) to be linked to the pyroclastic structure of soils. In this regard, the same authors proposed a bimodal lognormal function to describe soil hydraulic properties, taking into account the structure of pyroclastic soils in permeability functions on the basis of an experimental program performed on natural samples from Campania.

For the same point (point A along the slope) Fig. 12b shows the corresponding evolution of the safety factor. As expected, the minimum values were obtained in wet periods, albeit always higher than 1 (as confirmed by the absence of landslides).
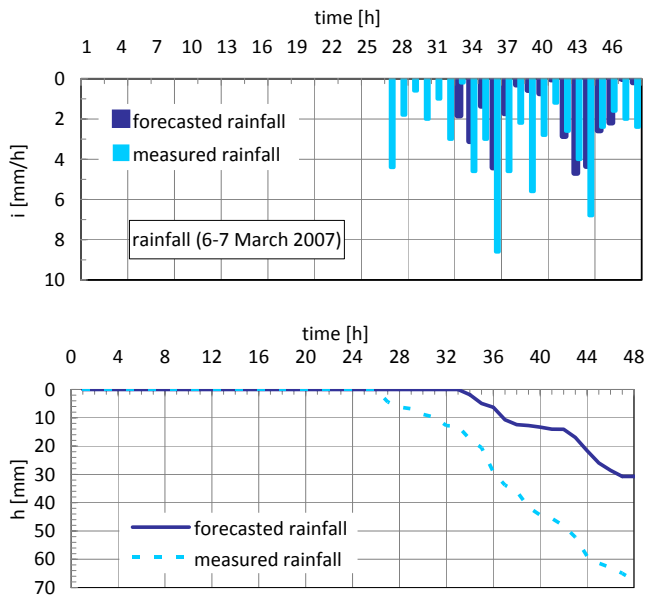
7.2　Test cases

Having calibrated the hydrological and geotechnical models, the "simulation chain" was "closed" by the three tests. The tests consisted of numerical simulations of the effects of the rainfall forecast in the 48/120 h after the three selected dates, substituting the recorded rainfall with the downscaled forecast rainfall derived from the MRI module. The initial condition in terms of suction and volumetric water content was derived from numerical simulation presented in the previous section (Fig. 12).

The selected dates were:

1. 3 April 2007 ($\Delta t = 48$ h) (Fig. 14);

2. 6 March 2007 ($\Delta t = 48$ h) (Fig. 15);

3. 6 February 2007 ($\Delta t = 120$ h) (Fig. 16).

In the first and second cases, the simulation period was 48 h; in the third case it was 120 h. Figure 17 shows a plain representation of the downscaled predicted rainfall obtained with the MRI module during the first test case. As described in Sect. 3.2, input data was obtained by MRI (physical desegregation of precipitation with topographical variables) and the residual was interpolated by the RBF method. The topographic variables utilized for desegregation were: elevation,
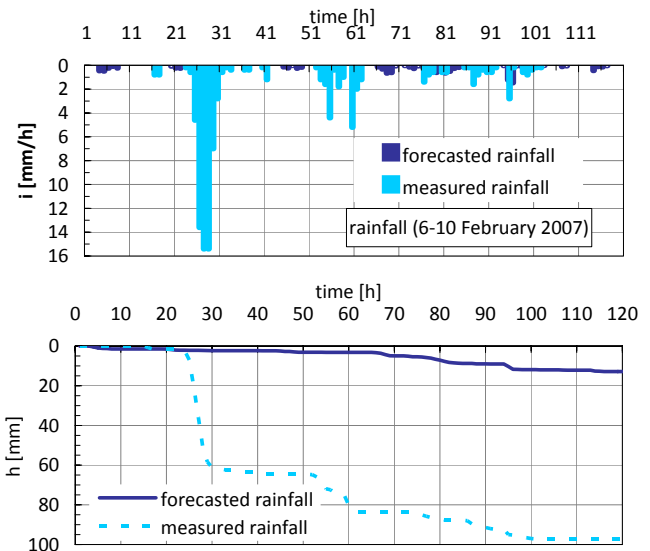
Fig. 15. Second test case: hourly rain intensity and cumulative rain height during 6–7 March 2007, evaluated at points A in the site of Cervinara.

Fig. 16. Third test case: hourly rain intensity and cumulative rain height during 6–10 February 2007, evaluated at points A in the site of Cervinara.

slope and aspect. The event lasted slightly more than one day and its paroxysmal phase was expressed on the second day: the rainfall began to take on appreciable values after 1 a.m., on 4 April 2007 and values greater than $5\,\mathrm{mm\,h^{-1}}$ were recorded during the second day.

In the first and second tests (Figs. 14 and 15), cumulative rainfall was about 20–30 mm but, in the first case, the rain was distributed over 34 h while in the second case within a much shorter period (15 h). The third case (Fig. 16) corresponds to a predicted rainfall of lower cumulative height (12 mm) distributed over a longer period (120 h). Comparison between measured (from pluviometric measurements at point A) and forecast rainfall reveals a qualitative agreement.

The Cervinara slope response predicted by the IMOD-3-D module is reported in Figs. 18 to 23. Figures 18, 20 and 22 show the results of the numerical simulation of the infiltration process in terms of safety factor using the output of the MRI module as a boundary condition at the ground surface and the results of numerical simulation (calibration step) reported in Fig. 12 as the initial condition. As expected, a strong reduction in the safety factor occurs only in the shallowest portion of the deposit (from the ground surface up to the depth of about 40–60 cm). The effects are negligible at greater depths. Similar information can be obtained from Figs. 19, 21 and 23 in which, for point A located along the slope, the same simulations are analysed in terms of capillary height (Ψ), volumetric water content (θ_w) and safety factor profiles.

Comparing the three tests it may be observed that:

1. the wetting front depth is influenced by the duration of the event: in the third case (DT = 120 h) there is a strong reduction in capillary height of up to 60–80 cm while in the second case (DT = 15 h of effective rain for 48 h of observations) the maximum depth reached by the infiltration process is about 36 cm. This clearly influences the depth at which the safety factor reduction is non-negligible.

2. the final value of safety factor is lower for test case 1 where rainfall had a greater cumulative height, starting from initial conditions with higher volumetric water content (lower capillary height).

In all three tests our "simulation chain" was successful in providing information about the link between predicted rainfall and slope response (at slope scale) as it considered the spatial and temporal distribution of predicted rainfall, soil properties (in saturated and unsaturated conditions) and the initial and boundary conditions (provided by the numerical simulation initialized from monitoring).

8   Conclusions

This paper set out to propose a Multidisciplinary Decision Support System (MDSS) as an approach to manage rainfall-induced shallow landslides of the flow-type (flowslides) in pyroclastic deposits. What ensured the robustness of the MDSS is its core based on advanced hydrological and geotechnical characterization which stem from laboratory
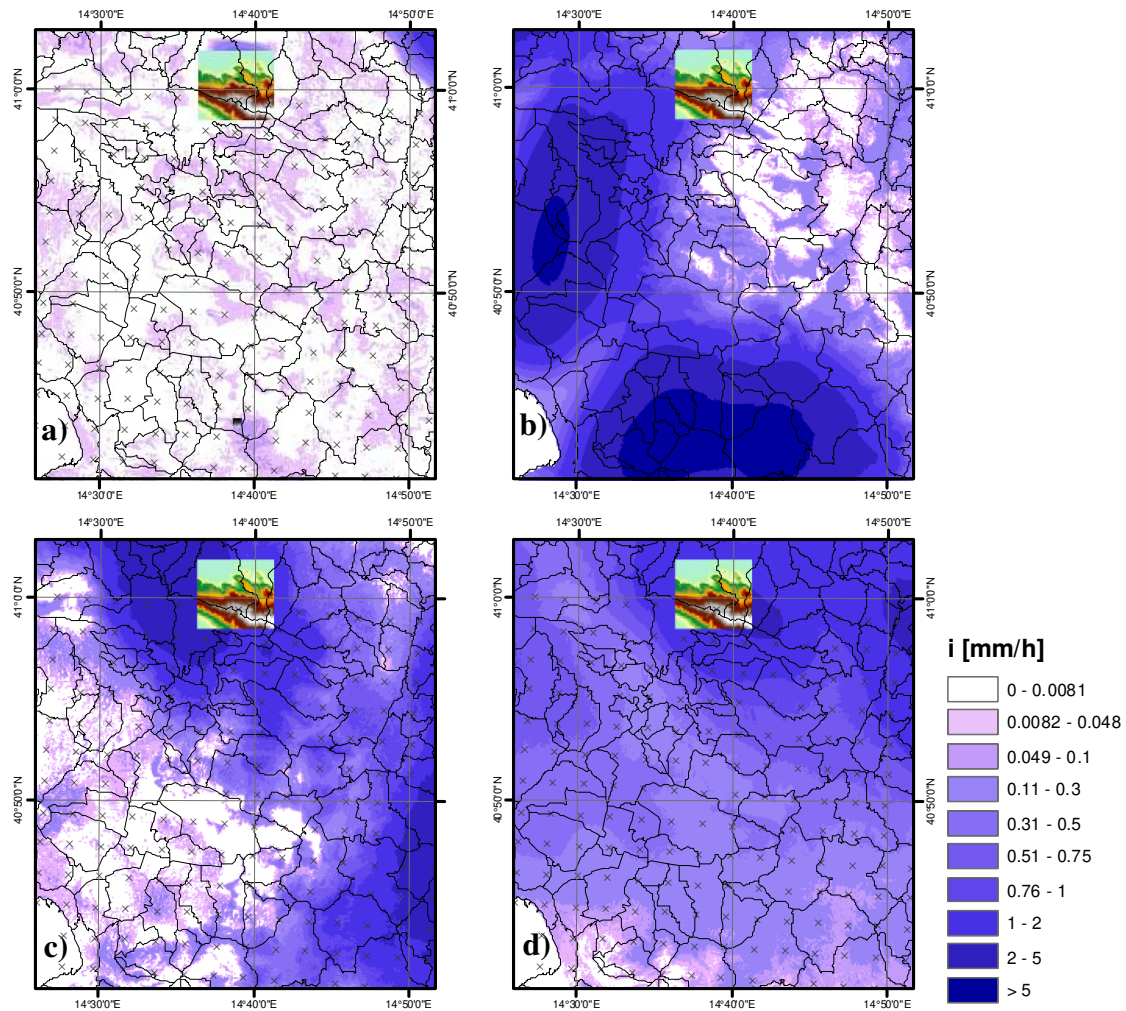
Fig. 17. Forecasted rainfall of 4 March 11 by MRI downscaling module; **(a)** time = 0; **(b)** time = 1 h; **(c)** time = 5 h; **(d)** time = 22 h.

and in situ investigation taking into account the real nature of soil.

In the Cervinara case it was possible to reproduce the slope response in terms of the variables which are necessary both to describe instability phenomena and the eventual evolution into a flowslide. The simulated trends of suction and volumetric water contents sufficiently reproduce, in a two-year monitoring program, the results obtained in wet periods. Instead, the results obtained in dry periods are only of a qualitative kind. This is the effect of the combination of simplified assumptions on evaporation flux applied in the model and biased estimations of hydraulic conductivity that cannot reproduce the true structure of pyroclastic soils.

As a future development, one of our aims is to implement the characteristic curves proposed by Romano et al. (2011) within our MDSS, in order to take into account the pyroclastic structure of soils. This could enhance the reliability of the estimation of hydraulic conductivity and of infiltration processes.

In accordance with the Prime Minister's Directive (2004), the Italian version of COSMO-LM (LAMI) is the reference model for the Italian Civil Protection. Our MDSS allows compliance with the Directive, since the forecasts provide the input for hydrological and geotechnical models initialized on the basis of the monitoring results.

The outputs of our MDSS, mainly warning maps and spatial distribution of water content, suction and degree of saturation, are necessary to understand the possibility of instability phenomena and post-failure evolution into flowslides. Such outputs may helpfully exclude the cases of landslides that will not evolve into catastrophic flowslides and allow the authorities involved in land management to reduce both the cases of "false" and "missed" alarms.
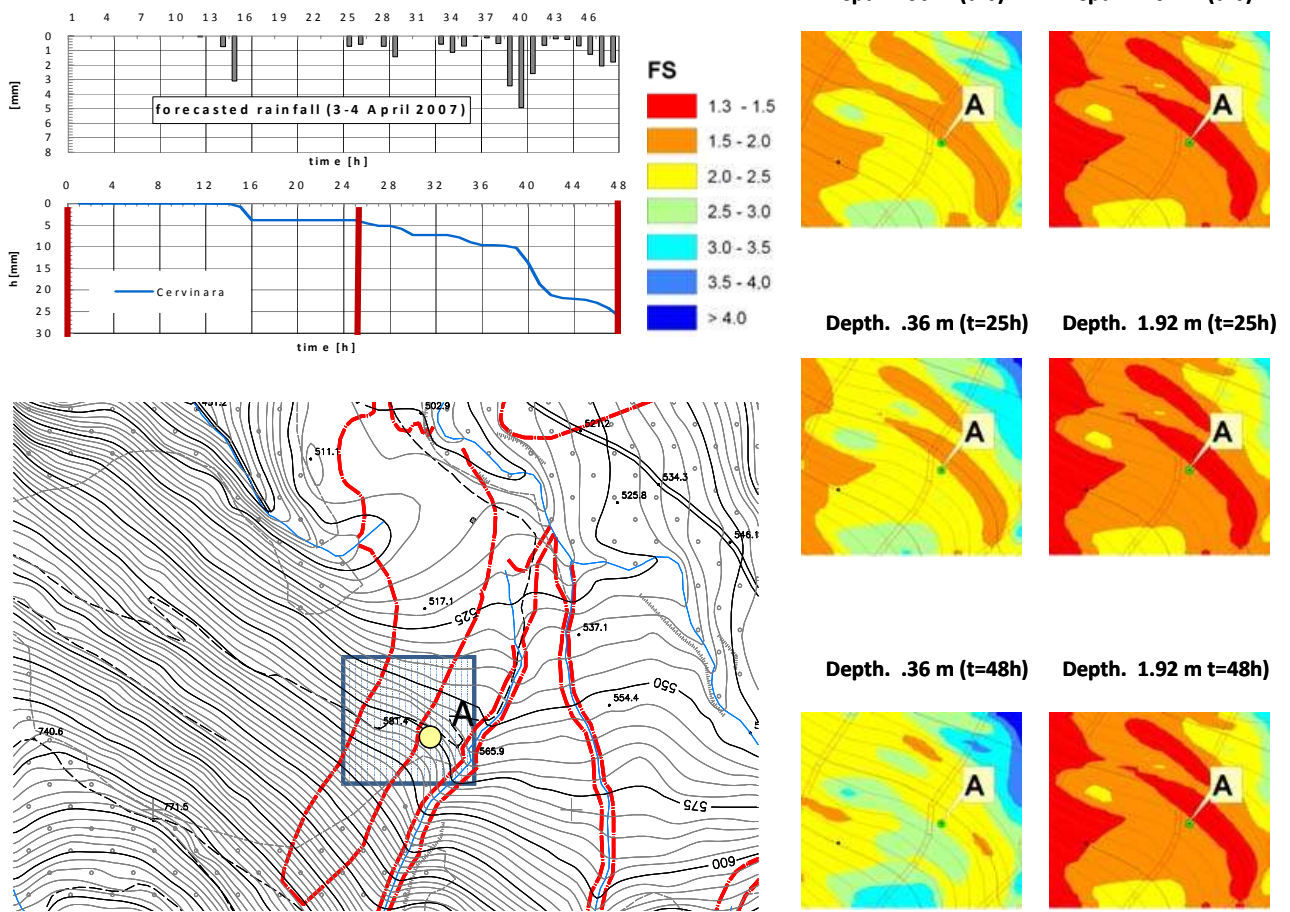
Cervinara test case : 3-4 April 2007

Fig. 18. First test case: distribution of safety factors vs. time at depths of 0.36 m and 1.92 m in the selected area.
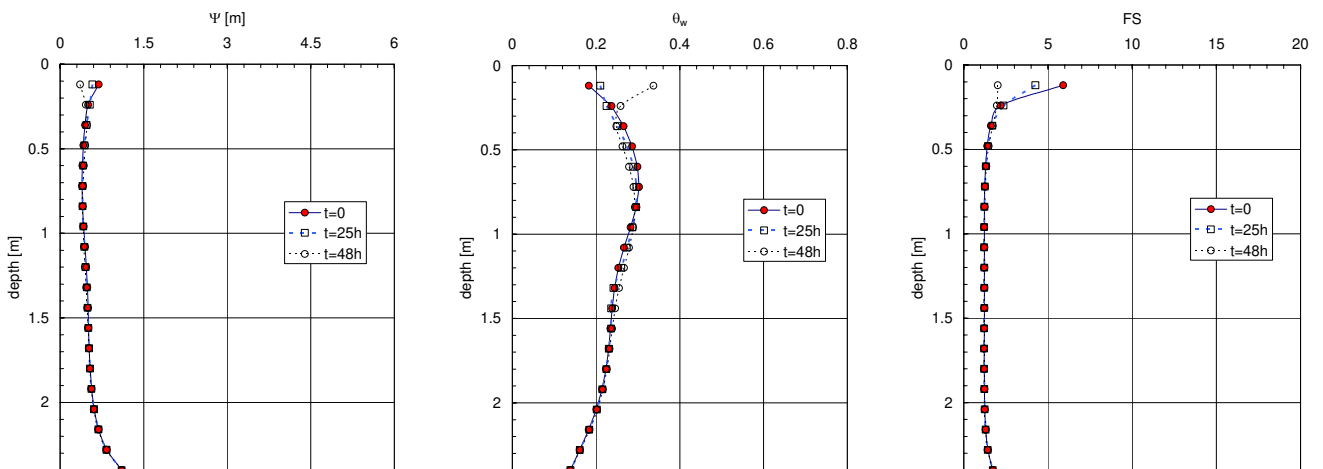

Fig. 19. First test case: capillary height, volumetric water contents and safety factors profiles at point A.
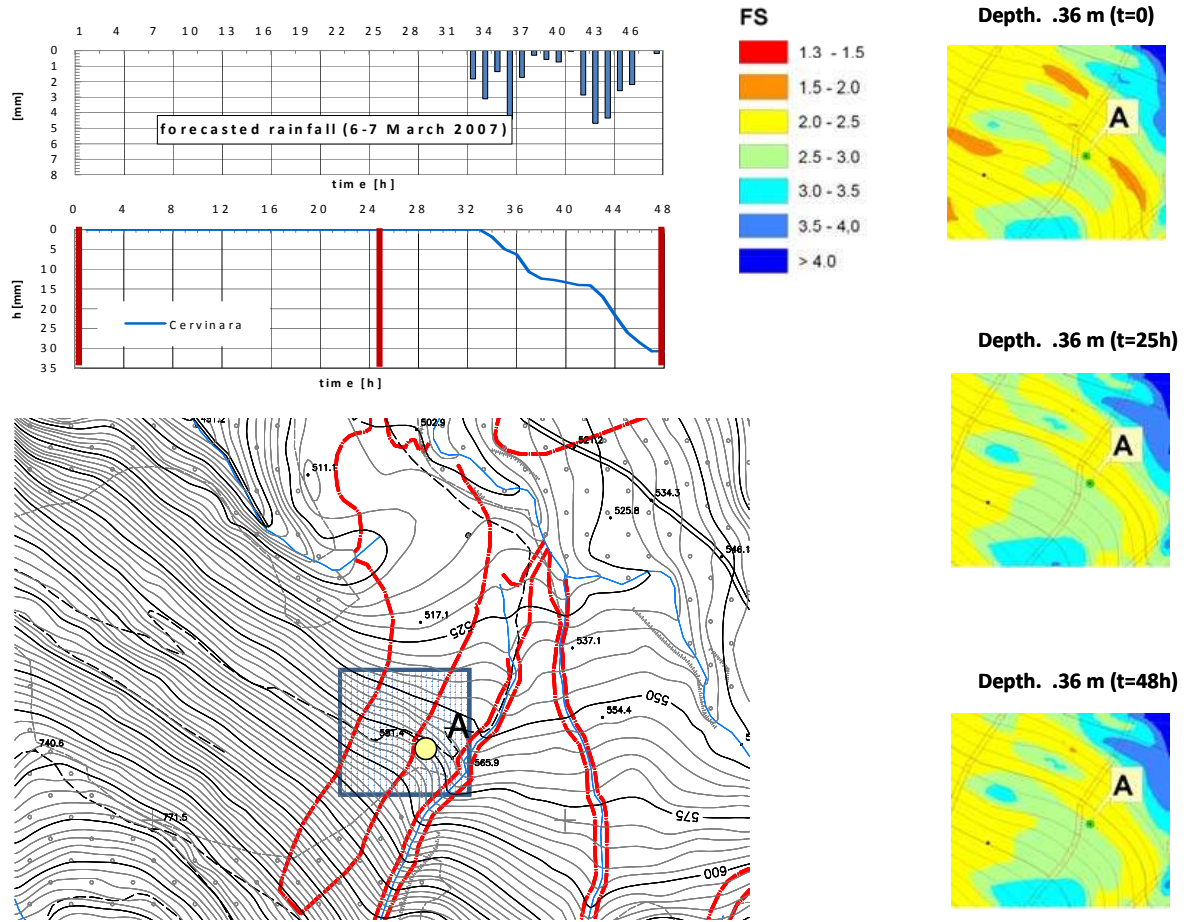
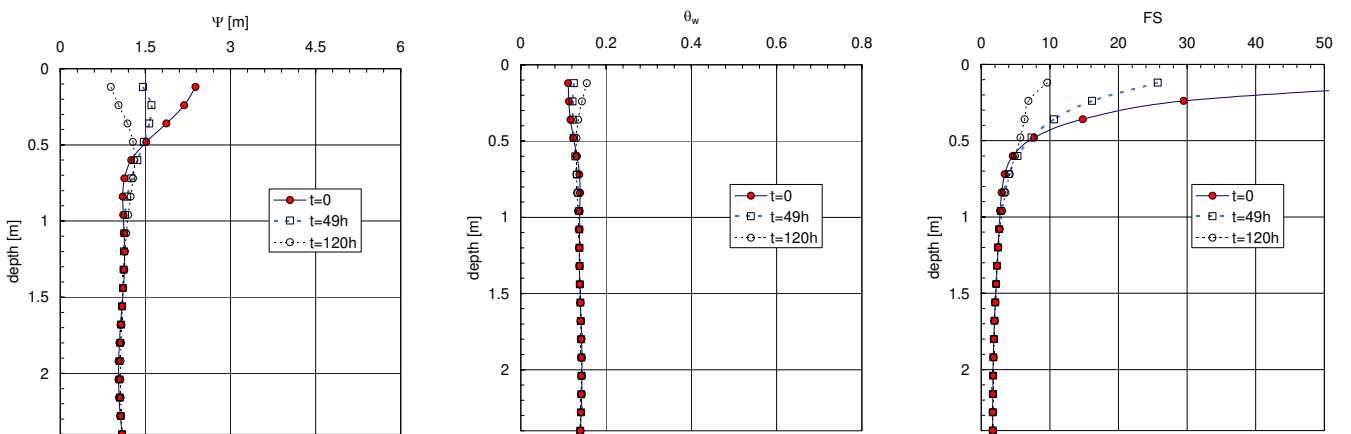**Fig. 20.** Second test case: distribution of safety factors vs. time at depths of 0.36 m in the selected area.
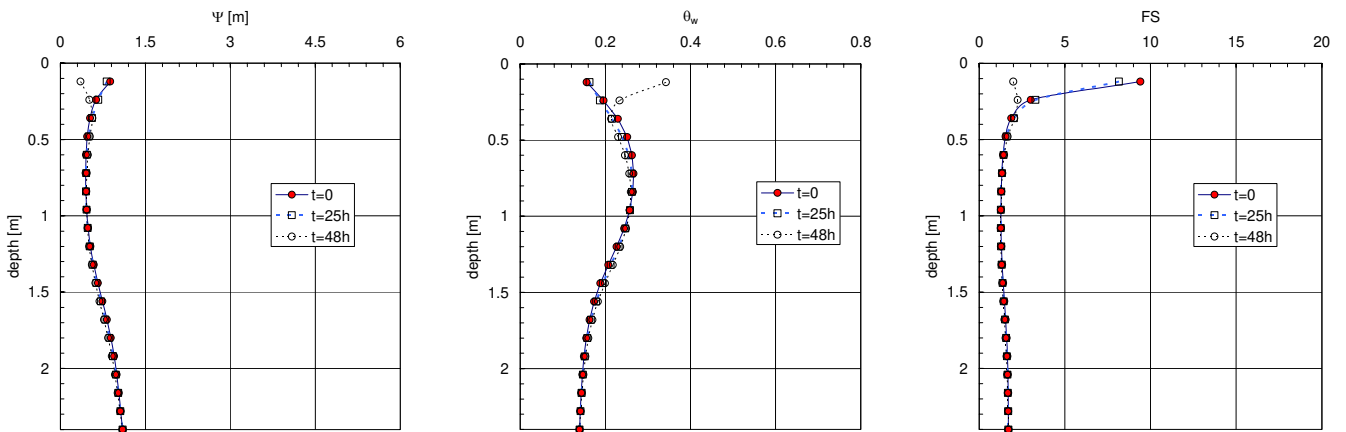
Fig. 21. Second test case: capillary height, volumetric water contents and safety factors profiles at point A.
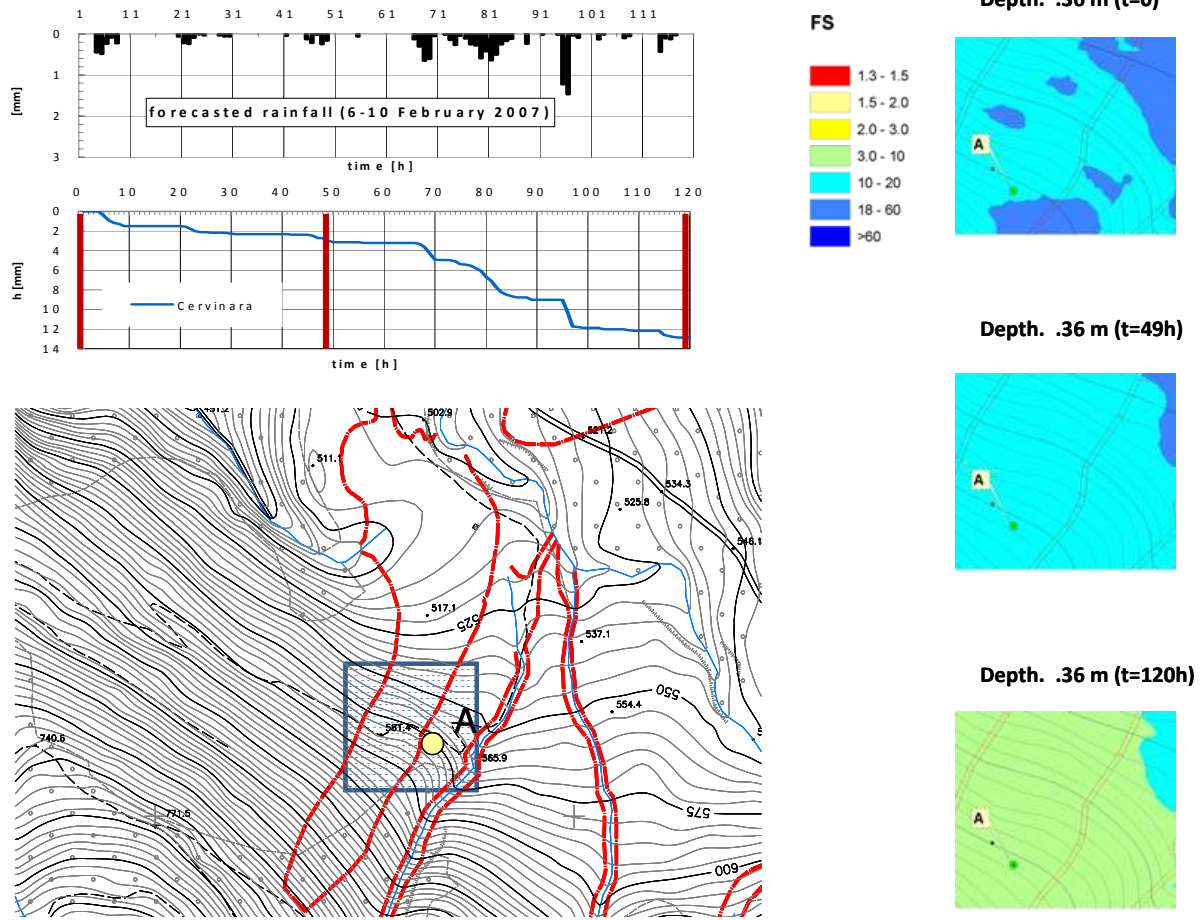
Fig. 22. Third test case: distribution of safety factors vs. time at depths of 0.36 m in the selected area.

Fig. 23. Third test case: capillary height, volumetric water contents and safety factors profiles at point A.

References

Agnew, M. D. and Palutikof, J. P.: GIS-based construction of base line climatologies for the Mediterranean using terrain variables, Climate Res., 14, 115–127, 2000.

Alexander, E. D.: Vulnerability to landslides, in: Landslide risk assessment, edited by: Glade, T., Anderson, M. G., and Crozier, M. J., John Wiley, 175–198, 2005.

Antofie, T. E.: Research Activity on Statistical Downscaling for Precipitation, Research Paper RP0057, Centro Euro-Mediterraneo per i Cambiamenti Climatici (CMCC), available at: http://www.cmcc.it/publications-meetings/publications/research-apers/rp0057-isc-02-2009, 2009.

Baillargeon, G.: Probabilité's Statistiques et Techniques de Régression (Statistical Probabilities and Regression Techniques), Editions SMG, 631 pp., 1989.

Baum, R. L., Savage, W. Z., and Godt, J. W.: TRIGRS – a FORTRAN program for transient rainfall infiltration and grid-based regional slope-stability analysis, US Geological Survey Open-File Report 02-0424, 2002.

Brooks, R. H. and Corey, A. T.: Hydraulic properties of porous media, Hydrology Paper N.3, Colorado State Univ., Fort Collins, Colorado, 1964.

Burrough, P. A. and McDonnell, R. A.: Principles of Geographical Information Systems, Oxford University Press, Oxford, 1998.

Cardinali, M., Reichenbach, P., Guzzetti, F., Ardizzone, F., Antonini, G., Galli, M., Cacciano, M., Castellani, M., and Salvati, P.: A geomorphological approach to the estimation of landslide hazards and risks in Umbria, Central Italy, Nat. Hazards Earth Syst. Sci., 2, 57–72, doi:10.5194/nhess-2-57-2002, 2002.

Carrara, A. and Guzzetti, F. (Eds): Geographical information systems in assessing natural hazards, Kluwer Dordrecht, 353 pp., 1995.

Carrara, A. and Merenda, L.: Metodologia per un censimento degli eventi franosi in Calabria, 1974.

Carrara, A., Cardinali, M., Detti, R., Guzzetti, F., Pasqui, V., and Reichenbach, P.: GIS Techniques and statistical models in evaluating landslide hazard, Earth Surf. Process. Land., 16, 427–445, 1991.

Carrara, A., Cardinali, M., Guzzetti, F., Reichenbach, P.: GIS technology in mapping landslide hazard, in: Geographical Information Systems in Assessing Natural Hazards, edited by: Carrara, A. and Guzzetti, F., Kluwer Academic Publishers, 135–175, 1995.

Cascini, L., Guida, D., Romanzi, G., Nocera, N., and Sorbino, G.: A preliminary model for the landslides of May 1998 in Campania Region, In: Proc. 2nd Int. Symp. The Geotechnics of Hard Soils-Soft Rocks, edited by: Evangelista, A. and Picarelli, L., Napoli, 3, 1623–1649, 2000.

Cascini, L., Bonnard, Ch., Corominas, J., Jibson, R., and Montero-Olarte, J.: Landslide hazard and risk zoning for urban planning and development, edited by: Hungr, O., Fell, R., Couture, R., and Eberthardt, E., in: Landslide Risk Management, Taylor and Francis, London, 199–235, 2005.

Cascini, L., Coumo, S., Pastor, M., and Sorbino, M.: Modeling of rainfall-induced shallow landslide of flow-type, J. Geotech. Geoenviron. Eng. ASCE, 136, 85–98, 2010.

Cascini, L., Cuomo, S., and Della Sala, M.: Spatial and temporal occurrence of rainfall-induced shallow landslides of flow type: A case of Sarno-Quindici, Italy, Geomorphology, 126, 148–158, 2011.

Chung, C.-J. F. and Fabbri, A. G.: Probabilistic prediction models for landslide hazard mapping, Photogramm. Eng. Rem. S., 65, 1389–1399, 1999.

Clark, T. L.: A small-scale dynamic model using a terrain-following coordinate transformation, J. Comput. Phys., 24, 186–215, 1977.

Corominas, J., Copons, R., Vilaplana, J. M., Altimir, J., and Amigó, J.: Integrated landslide susceptibility analysis and hazard assessment in the Principality of Andorra, Nat. Hazards, 30, 421–435, 2003.

Crosta, G. B. and Dal Negro, P.: Observations and modelling of soil slip-debris flow initiation processes in pyroclastic deposits: the Sarno 1998 event, Nat. Hazards Earth Syst. Sci., 3, 53–69, doi:10.5194/nhess-3-53-2003, 2003.

Crosta, G. B. and Frattini, P.: Distributed modelling of shallow landslides triggered by intense rainfall, Nat. Hazards Earth Syst. Sci., 3, 81–93, doi:10.5194/nhess-3-81-2003, 2003.

D'Odorico, P., Porporato, A., and Ridolfi, L.: Transition between stable states in the dinamics of soil development, Geophys. Res. Lett., 28, 595–598, 2001.

Damiano, E. and Olivares, L.: The role of infiltration processes in steep slopes stability of pyroclastic granular soils: laboratory and numerical investigation. Natural Hazards, Journal of the Inter. Society for the Prevention and Mitigation of Natural Hazards, Springer Netherlands, 52, 329–350, 2010.

Damiano, E., Olivares, L., and Picarelli, L.: Steep-slope monitoring in unsaturated pyroclastic soils, Eng. Geol., in press, 2012.

Davies, H.: A lateral boundary formulation for multi-level prediction models, Quart. J. Roy. Met. Soc., 102, 405–418, 1976.

Davies, H.: Limitation of some common lateral boundary conditions used in regional NWP models, Mon. Weather Rev., 111, 1002–1012, 1983.

De Graff, J. and Canuti, P.: Using isopleth mapping to evaluate landslide activity in relation to agricultural practices, Bull. Assoc. Eng. Geol., 38, 61–71, 1988.

Del Prete, M., Guadagno, F. M., and Hawkins, A. B.: Preliminary report on the landslides of 5 May 1998, Campania, southern Italy, Bull. Eng. Geol. Environ., 57, 113–129, 1998.

Di Crescenzo, G. and Santo, A.: Debris slides-rapid earth flows in the carbonate massifs of the Campania region (Southern Italy): morphological and morphometric data for evaluating triggering

susceptibility, Geomorphology, 66, 255–276, 2005.

Doms, G. and Schattler, U.: The non-hydrostatic limited area model LM (Lokal Model) of DWD, Part I, Scientific documentation, Deutscher Wetterdienst, Germany, , available at: http://cosmo-model.cscs.ch, 1999.

Doms, G. and Schattler, U.: A Description of the Nonhydrostatic Regional Model LM, Deutscher Wetterdienst Deutscher Wetterdienst, Germany, 1, 1–130, 2002.

Doms, G. and Shatteler, U.: A Description of the Nonhydrostatic Regional Model LM Part I: Dynamics and Numerics, available at: http://www.cosmo-model.org/content/model/documentation/core/default.htm#p1, 2011.

Doms, G., Forstner, J., Heise, E., Herzog, H.-J., Raschendorfer, M., Schrodin, R., Reinhardt, Th., and Vogel, G.: A description of the Nonhydrostatic Regional Model LM, Part II: Physical parameterization, available at: http://www.cosmo-model.org, 2005.

Evans, S. G., Cruden, D. M., Bobrowsky, P. T., Guthrie, R. H., Keegan, T. R., Liverman, D. G. E., and Perret, D.: Landslide risk assessment in Canada: a review of recent developments, in: Landslide Risk Management, edited by: Hungr, O., Fell, R., Couture, R., and Eberthardt, E., Taylor and Francis, London, 351–363, 2005.

Fell, R., Walker, B. F., and Finlay, P. J.: Estimating the probability of landsliding, Proc. 7th Australian New Zealand Conference on Geomechanics, Adelaide, Institution of Engineers Australia, Canberra, 304–311, 1996.

Fell, R., Corominas, J., Bonnard, C., Cascini, L., Leroi, E., and Savage, W. Z.: Guidelines for landslide susceptibility, hazard and risk zoning for land-use planning, Eng. Geol., 102, 99–111, 2008.

Fredlund, D. G. and Rahardjo, H.: Soil Mechanics for Unsaturated Soils, Wiley-Interscience Publication, John Wiley & Sons, Inc., 1993.

Gamper, C. D., Thöni, M., and Weck-Hannemann, H.: A conceptual approach to the use of Cost Benefit and Multi Criteria Analysis in natural hazard management, Nat. Hazards Earth Syst. Sci., 6, 293–302, doi:10.5194/nhess-6-293-2006, 2006.

Gardner, W. R.: Some steady state solutions of the un-saturated moisture flow equation with application to evaporation from water table, Soil Sci., 85, 228–232, 1958.

Gorsevski, P. V., Gessler, P. E., and Jankowski, P.: Integrating a fuzzy k-means classifications and a Bayesian approach for spatial prediction of landslide hazard, J. Geogr. Syst., 5, 223–251, 2003.

Greco, R. and Guida, A.: Field measurements of topsoil moisture profiles by vertical TDR probes, J. Hydrol., 348, 442–451, 2008.

Greco, R., Guida, A., Damiano, E., and Olivares, L.: Soil water content and suction monitoring in model slopes for shallow flowslides early warning applications, Phys. Chem. Earth, 35, 127–136, 2010.

Guadagno, F., Martino, S., and Scarascia Mugnozza, G.: Influence of man-made cuts on the stability of pyroclastic covers (Campania, southern Italy): a numerical modelling approach, Environ. Geol. V, 43, 371–384, 2003.

Guiso, L. and Terlizzese, D.: Economia dell'incertezza e dell'informazione, edited by: Hoepli, U., Milano, 1994.

Guzzetti, F.: Landslide fatalities and evaluation of landslide risk in Italy, Eng. Geol., 58, 89–107, 2000.

Guzzetti, F.: Landslide hazard and risk assessment: Concepts, methods and tools for the detection and mapping of land-

slides, for landslide susceptibility zonation and hazard assessment, and for landslide risk evaluation, Dissertation zur Erlangung des Doktorgrads (dr. rer. nat.) der Mathematisch-Naturwissenschaftlichen Fakultät der Rheinischen Friedrich-Wilhelms-Univestität Bonn, available at: http://hss.ulb.uni-bonn.de/2006/0817/0817.htm, 1, 399 pp., 2006.

Guzzetti, F., Stark, C. P., and Salvati, P.: Evaluation of Flood and Landslide Risk to the Population of Italy, Environ. Manage., 36, 15–36, 2005.

Hanoch, G. and Levy, H.: The efficiency analysis of choices involving risk. Review of Economic Studies, vol. 36, pp. 335-346, 1969.

Heise, E., Ritter, B., and Schrodin, R.: Technical Report No. 9 July 2006, Operational Implementation of theMultilayer Soil Model, available at: http://www.dwd.de/bvbw/generator/DWDWWW/Content/Forschung/FE1/Veroeffentlichungen/Download/Cosmo_tech_rep/costr9_en,templateId=raw,property=publicationFile.pdf/costr9_en.pdf, 2006.

Hollingworth, R. and Kovacs, G. S.: Soil slumps and debris flows: prediction and protection, Bull. As. Eng. Geol., 18, 17–28, 1981.

Hungr, O., Evans, S. G., and Hazzard, J.: Magnitude and frequency of rock falls and rock slides along the main transportation corridors of southwest British Columbia, Can. Getech. J., 36, 224–238, 1999.

IUGS Working Group on Landslides, Committee on Risk Assessment: 1997, Quantitative risk assessment for slopes and landslides – The state-of-the-art, in: Landslide Risk Assessment, edited by: Cruden, D. M. and Fell, R., 3–12, 1997.

Iverson, R.: Landslide Triggering by Rain Infiltration, Water Resour. Res., 36, 1897–1910, 2000.

Leroueil, S.: Geotechnics of slopes before failure, in: Proc. IX Int. Symp. on Landslides: evaluation and stabilization, edited by: Lacerda, W. A., Ehrlich, M., Fontoura, S. A. B., and Sayão, A. S. F., Rio de Janeiro, June 2004, 863–884, 2004.

Lida, T.: Theoretical research on the relationship between return period of rainfall and shallow landslides, Hydrol. Process, 18, 739–756, 2004.

Marschak, J. and Radner, R.: Economic theory of teams, Yale Unuversity Press, New Haven, 1972.

McCalpin, J.: Preliminary age classification of landslides for inventory mapping, Proc. 21st Annual Engineering Geology andSoils Engineering Symposium, Moscow, 99–111, 1984.

Montgomery, D. R. and Dietrich, W. E.: A physically based model for the topographic control on shallow landsliding, Water Resour. Res., 30, 1153–1171, 1994.

Montgomery, D. R., Wright, R. H., and Booth, T.: Debris flow hazard mitigation for colluvium-filled swales, Bull. Assoc. Eng. Geol., 28, 303–323, 1991.

Ninyerola, M., Pons, X., and Roure, J. M.: A methodological approach of climatological modeling of air temperature and precipitation through GIS techniques, Int. J. Climatol., 20, 1823–1841, 2000.

Olivares, L.: Static liquefaction: an hypothesis for explaining transition from slide to flow in pyroclastic soils, Proc. ISSMGE CT-11, Transition from slide to flow: mechanisms and remedial measures, Trabzon, August 2001, 2001.

Olivares, L. and Damiano, E.: Post-failure mechanics of landslides: laboratory investigation of flowslides in pyroclastic soils, J. Geotech. Geoenviron. Eng. ASCE, 133, 51–62, 2007.

Olivares, L. and Picarelli, L.: Occurrence of flowslide in soils of pyroclastic origin and considerations for landslide hazard mapping, The Fourteenth Southeast Asian Geotechnical Conference; 10–14 December 2001, Hong Kong, 1, 881–886, 2001.

Olivares, L. and Picarelli, L.: Shallow flowslides triggered by intense rainfalls on natural slopes covered by loose unsaturated pyroclastic soils, Géotechnique, 53, 283–288, 2003.

Olivares, L. and Tommasi, P.: The role of suction and its changes on stability of steep slopes in unsaturated granular soils, Proc. X Int. Symp. on Landslides and Engineered Slopes – Xi'an, China, Nederland/Taylor and Francis Group, London, ISBN 978-0-415-41196-7, 1, 203–216, 2008.

Olivares, L., Andreozzi, L., Damiano, E., Avolio, B., and Picarelli, L.: Hydrologic response of a steep slope in unsatured pyroclastic soils, Int. Conf. on: Fast Slope Movements-Prediction and Prevention for Risk Mitigation IC-FSM2003, Napoli, Maggio, 11–13, 2003, Patron Editore, Bologna, 1, 391–398, 2003.

Olivares, L., Damiano, E., Greco, R., Zeni, L., Picarelli, L., Minardo, A., Guida, A., and Bernini, R.: An Instrumented Flume to Investigate the Mechanics of Rainfall-Induced Landslides in Unsaturated Granular Soils, Geotech. Test. J., 32, 1–11, ISSN:0149-6115, 2009.

Phillips, N. A.: A coordinate system having some special advantages for numerical forecasting, J. Meteorol., 14, 184–185, 1957.

Picarelli, L., Olivares, L., Andreozzi, L., Damiano, E., and Lampitiello, S.: A research on flowslides induced by rainfall in unsaturated soils of pyroclastic origin, IX International Symposium on Ladslides-Rio De Janeiro, Swets & Zeitlinger, Lisse A.A. Balkema, Rotterdam, 2, 1497–1506, 2004.

Picarelli, L., Oboni, F., Evans, S. G., Mostyn, G., and Fell, R.: Hazard characterization and quantification, in: Landslide Risk Management, edited by: Hungr, O., Fell, R., Couture, R., and Eberhardt, E., Taylor and Francis, London, 27–62, 2005.

Picarelli, L., Olivares, L., and Avolio, B.: Zoning for flowslide and debris flow in pyroclastic soils of Campania Region based on "infinite slope" analysis, Eng. Geol., 102, 132–141, doi:10.1016/J.engeo.2008.03.015, 2008a.

Picarelli, L., Olivares, L., Comegna, L., and Damiano, E.: Mechanical aspects of flow-like movements in granular and fine-grained soils, Rock Mech. Rock Eng., Springer, Nederland, , 41, 179–197, doi:10.1007/s00603-007-0135x, 2008b.

Picarelli, L., Santo, A., Di Crescenzo, G., and Olivares, L.: Macro-zoning of areas susceptible to flowslide in pyroclastic soils in Campania Region, Proc. X International Symposium on Ladslides and Enginneered Slopes – Xi'an – China, Swets & Zeitlinger, Lisse A.A., Balkema, Rotterdam, ISBN 978-0-415-411195.0, 2, 1951–1958, 2008c.

Pratt, J.: Risk aversion in the small and in the large, Econometrica, 32, 122–136, 1964.

Prime Minister's Directive: Direttiva del Presidente del consiglio del 27.02.2004, Indirizzi operativi per la gestione organizzativa e funzionale del sistema di allertamento nazionale e regionale per il rischio idrogeologico ed idraulico a fini di protezione civile, n. 39 alla Gazzetta Ufficiale, n.59 dell'11 marzo 2004, 2004 (in Italian).

Revellino, P., Hungr, O., Guadagno, F. M., and Evans, S. G.: Velocity and runout simulation of destructive debris flows and debris avalanches in pyroclastic deposits, Campania Region, Italy, Environ. Geol., 45, 295–311, 2004.

Romano, N., Nasta, P., Severino, G., and Hopmans, J. W.: Using Bimodal Lognormal Functions to Describe Soil Hydraulic Properties, Soil Phys. Soil Sci. Soc. Am. J., 75, 468–480, 2011.

Rose, A. and Lim, D.: Business interruption losses from natural hazards: conceptual and methodological issues in the case of the Northridge earthquake, Environ. Hazards, 4, 1–14, 2002.

Rosso, R., Rulli, M. C., and Vannucchi, G.: A physically based model for the hydrologic control on shallow landsliding, Water Resour. Res., 42, W06410, doi:10.1029/2005WR004369, 2006.

Rothschild, M. and Stiglitz, J.: Increasing risk: I. A definition, J. Economic Theory, 2, 225–243, 1970.

SafeLand Project: Living with landslide risk in Europe: Assessment, effects of global change, and risk management strategies, available at: http://www.cmcc.it/ricerca/progetti/safeland, 2011.

Savage, W. Z., Godt, J. W., and Baum, R. L.: Modeling timedependent areal slope stability, in: Landslides – Evaluation and Stabilization, edited by: Lacerda, W. A., Erlich, M., Fontoura, S. A. B., and Sayao, A. S. F., Proceedings of the 9th International Symposium on Landslides, Rotterdam, Balkema, 1, 23–36, 2004.

Shattler, U.: Preprocessing: Initial and Boundary Data for the COSMO Model, available at: http://www.cosmo-model.org/content/model/documentation/core/cosmoInt2lm.pdf, 2009.

Torrisi, L.: COSMO Newsletter No. 5: A new option of the upper level Rayleigh damping, available at: http://cosmo-model.cscs.ch/content/model/documentation/newsLetters/newsLetter05, 2005.

Trentmann, J., Keil, C., Salzmann, M., Barthlott, C., Bauer, H. S., Schwitalla, T., Lawrence, M. G., Leuenberger, D., Wulfmeyer, V., Corsmeier, U., Kottmeier, C., and Wernli, H.: Multi-model simulations of a convective situation in low-mountain terrain in central Europe, Meteorol. Atmos. Phys., 103, 95–103, 2009.

Van Genuchten, M. Th.: A closed-form equation for predicting the hydraulic conductivity of unsaturated soil, Soil Sci. Soc. Am. J., 44, 615–628, 1980.

Varnes, D. J.: Landslide Hazard Zonation: A Review of Principles and Practice, UNESCO Press, Paris, 9–63, 1984.

Vaunat, J. and Leroueil, S.: Analysis of post-Failure Slope Movements within the framework of Hazard and Risk Analysis, Nat. Hazards, 26, 83–109, 2002.

Vigier, M.: Mèthodes d'Assurance Qualité–Fiabilité et d'Expérimentation (Quality Insurance Methods–Reliability and Experiments), Collection Universite' de Compiègne, 398 pp., 1981.

Von Neumann, J. and Morgenstern, O. Theory of games and economic behaviour, Princeton University Press, Princeton, New Jersey, 1944.

Wieczorek, G. F.: Preparing detailed landslide-inventory map for hazard evaluation reduction, Bull. Assoc. Eng. Geol., 21, 337–342, 1984.